AN ABSTRACT OF THE THESIS OF

Anthony James Elliott for the degree of Master of Science in Nuclear Engineering presented on May 29, 2008.

Title: Radioxenon Generation using Highly Enriched Uranium

Abstract approved:

David M. Hamby

This work focuses on the generation and collection of four specific radioxenon isotopes; xenon-131m, xenon-133m, xenon-133 and xenon-135. These nuclides are created by fissioning a highly enriched uranium sample using a thermal neutron source from a university research reactor. The three main aspects of this work include:

(1) Conducting preliminary calculations of xenon fission products;
(2) Designing and constructing an apparatus for sample irradiation and gas delivery; and
(3) Generating xenon gas from a reusable apparatus that will allow for multiple radioxenon production events.

Also included in the following work is a comprehensive background on information pertaining to the works included. This information should aid

individuals unfamiliar in the nuclear field a background understanding of the topics discussed.

The preliminary calculations performed are used to find values such as flux, fission product percentages created, dose, as well as a range of other pertinent information. The calculations have been performed primarily to aid in the generation of the xenon isotopes, but also to obtain the necessary approvals to perform the irradiation experiment at Oregon State University.

The design section of this work includes detailed information on the fabrication of the apparatus used to generate the fission gas products. This includes blueprints, manufacturing techniques, parts list, as well as a final assembled apparatus figure to allow for easy reproduction of the system. The fission chamber device utilized for the irradiation of the HEU material is of a flange design constructed of aluminum. The entire system has been designed for irradiation outside the reactor bioshield, utilizing a neutron beamport adjacent to the reactor core.

This work also includes an analysis of the xenon isotopes created to verify the experimental success. Using the XEPHWICH detector developed at Oregon State University, the xenon isotopes were counted and identified for verification of activities and correct yield percentages. The generation system efficiency is also determined to account for system losses. With an accurate approximation on the generation efficiency, this fission gas generation system can also be used to create radioxenon isotopes for the calibration of specific detector designs.

Radioxenon Generation using Highly Enriched Uranium

by
Anthony James Elliott

A THESIS

submitted to

Oregon State University

in partial fulfillment of
the requirements for the
degree of

Master of Science

Presented May 29, 2008
Commencement June 2009

Master of Science thesis of Anthony James Elliott presented on May 29, 2008.

APPROVED:

Major Professor, representing Nuclear Engineering

Head of the Department of Nuclear Engineering and Radiation Health Physics

---

Dean of the Graduate School

I understand that my thesis will become part of the permanent collection of Oregon State University libraries. My signature below authorizes release of my thesis to any reader upon request.

Anthony James Elliott, Author

ACKNOWLEDGEMENTS

Firstly, I would like to thank Dr. David Hamby who allowed me to complete this work and pursue my degree under his guidance. His faith in me has allowed me to confidently achieve the goals of my work, while challenging me intellectually along the way.

Secondly, to Dr. Steve Reese for his guidance and help directly related to the regulations required to complete this process.

I would also like to acknowledge Scott Menn for his support in the operations of the project.

Also, I would like to thank Dr. Abi Farsoni for his work with the XEPHWICH, and the patience he has shown me for the prolonging delays occurred in the project.

I would also like to thank Todd Keller for helping me with the reactor approval process and design phases of my project.

Finally I would like to thank my friends and family for the support that they have shown me during the time I have spent working on this project.

TABLE OF CONTENTS

TABLE OF CONTENTS (Continued)

TABLE OF CONTENTS (Continued)

LIST OF FIGURES

LIST OF FIGURES (Continued)

LIST OF FIGURES (Continued)

LIST OF TABLES

LIST OF APPENDICES

LIST OF APPENDIX FIGURES

LIST OF APPENDIX TABLES

DEDICATION:

To my family.

RADIOXENON GENERATION USING HIGHLY ENRICHED URANIUM

1. INTRODUCTION

On the fateful morning of July 16th, 1945 the world changed in the blink of an eye with the dawn of the nuclear age. Since this historic day, nations have dedicated a plethora of resources to develop nuclear technologies. As arms races still continue and nonproliferation is in the forefront of many of the nuclear capable countries, technologies are being developed to help detect the use of nuclear weapons.

Radioxenon gas is one of the major byproducts from the fission of uranium. Above normal concentrations of xenon gas in the environment can help determine if nuclear fissioning has occurred from either reactors, or weapon detonations. The purpose of creating radioisotopes of xenon in the laboratory is to facilitate the calibration and characterization of detectors to identify the xenon isotopes that are created directly from fission. The radioxenon isotopes of interest for this experiment are xenon-131m, xenon-133m, xenon-133 and xenon-135.

The main objectives of this thesis work are to:

(1) Conduct preliminary calculations of xenon fission products;

(2) Design and construct an apparatus for sample irradiation and gas delivery; and

(3) Generate xenon gas from a reusable apparatus that will allow for multiple radioxenon production events.

Although this does seem straightforward, there are also many legal and health concerns with the irradiation of a foil of highly enriched uranium that must be considered as part of this work. Fissile material is usually not irradiated outside of the reactor core, thus special consideration was necessary in dealing with the aspect of potential fission byproduct releases to the environment. A discussion of the purity of the uranium foil will also help to identify the decision for the high enrichment compared to a lower enriched and easier to handle sample. Fortunately for the scope of the experiments conducted, the activity created was relatively small, in the picocurie range, for the xenon isotopes of interest.

The Xenon Phoswich (XEPHWICH) detector created in the radiation detection lab at Oregon State University is a newly designed and constructed detector that will allow the capture and identification of the xenon-131m, xenon-133m, xenon-133 and xenon-135 nuclides, as well as other key nuclides. The radioxenon isotopes were specifically chosen for detection due to their distinct energy emissions, as well as their inert properties. Xenon gas, a noble element, will not bond to other elements to create molecules, thus it will remain highly mobile and in its' pure form. This characteristic (mobility) allows for the gas to escape from normal containment situations, such as underground nuclear detonations, where other fission products would normally become trapped.

2. LITERATURE REVIEW

2.1. METHODS OF OBTAINING RADIOXENON

There are several distinctive ways of producing radioactive material. The first is to fission an element that has a high mass, such as uranium or plutonium, if there is a discernable way of removing the nuclides of interest. The other method is through activation of a stable lower-mass element to achieve the radioactive nuclide of interest. In the context of this work, xenon is the primary element that will be examined. Naturally occurring xenon comprises an extremely small fraction of Earth's atmosphere with a relative abundance fifty parts per billion (LANL, 2008). This number does not represent the even smaller fraction that radioxenon isotopes represent from both natural and artificial source.

2.1.1. FISSION

The method of obtaining radioactive xenon, or radioxenon, through the fission process is achievable through several methods. In all instances, the initial element must have an atomic mass great enough such that one of the fragments of fission can have an atomic mass equal to that of xenon. Xenon is naturally created as a byproduct of the spontaneous fission of uranium, thorium, plutonium and other heavy elements. The extremely long half-life and relatively small abundance

of these isotopes, in conjunction with the low yield of fission resulting in xenon, makes the natural occurring xenon scarce.

Radioxenon may also be created though the fission of isotopes of uranium, such as uranium-235. In this process, xenon may be obtained by placing uranium in a neutron rich environment, such as a nuclear reactor core, or near a neutron emitting source. This will cause the uranium to fission and create radioxenon as one of the fission byproducts. These byproducts can then be separated bearing the desired radioxenon.

2.1.2. ACTIVATION

The method of obtaining radioxenon through activation first requires the collection a of stable xenon isotope. This isotope is then bombarded with a neutron source, similar to that of the fission process. During this process, however, xenon nuclei will absorb a neutron, therefore changing the isotope. An example of this process could be demonstrated by creating xenon-135, from the stable xenon-134 isotope.

$$^{134}\mathrm{Xe} + {}^{1}n = {}^{135}\mathrm{Xe}$$

2.2. COMPREHENSIVE NUCLEAR TEST-BAN TREATY

The *Comprehensive Nuclear Test-Ban Treaty* (CTBT) was formed in 1996 under the supervision of the United Nations General Assembly. Since this time,

over 170 countries have become recognized member states of the treaty. The CTBT bans all nuclear weapon detonations and sets forth standards for the monitoring protocol to verify the adherence of the treaty.

Under the stipulations of the CTBT, a system of detectors must be established and deployed to monitor the atmosphere for relevant particulate matter. The monitoring system shall be capable of noble gas monitoring.[1]

Several monitoring systems have already been developed for the applications under the CTBT, and detector design is continually evolving to improve the capability to detect noble gas radionuclides. Newly developed detection systems are in need of xenon gas to help verify their capability required under the CTBT, and thus the need for a xenon generation system has been created. Under the CTBT, the minimal detection limit of a specific xenon isotope, xenon-133, must be no greater than 1 mBq/m³ (CTBT, 2008). This standard provides the generation guidelines for the radioxenon system.

2.3. PNNL-14338 GENERATION OF RADIOXENON ISOTOPES

After extensive review and investigation, the only published radioxenon generation method was retrieved from *Pacific Northwest National Laboratory* (PNNL). From this report and through discussion with the author, Justin

[1] The Comprehensive Nuclear-Test-Ban-Treaty states in its: Protocol to The Comprehensive Nuclear Test-ban Treaty, Part I, A. General Provisions, C. Radionuclide Monitoring, Section 10.

McIntyre, it was apparent that two methods have previously been used in the creation of fission-product radioxenon.

The first method involves utilization of the reactor facility at Washington State University. In this procedure, a small quartz vial containing a microgram quantity of uranium-235 was irradiated (McIntyre, 2003). The inherent problem in the generation of the gas in this method was that the vial had to be sacrificed to extract the fission gas and thus each sample had to be independently created, lending to variability in geometry of the irradiated device.

The second method of generation involved the irradiation of uranium oxide powder containing uranium-235. Although this method did allow for multiple generations using the identical system, the production time for each sample was several hours to several weeks (McIntyre, 2003). In this method, samples could not be easily created in short duration of each other. **Figure 1** and **Figure 2** depict the configuration and schematic, respectively, of this generation system. The neutron sources depicted in **Figure 1** were a combination of an 80 gram PuBe source and a 10 microgram californium-252 source with neutron fluxes of 8.8×10^8 [neutrons / cm²-s] and 2.8×10^7 [neutrons / cm²-s], respectively (McIntyre, 2003). Using this system, the approximately 25 mBq of xenon-133 and 50 Bq of xenon-135 were created after a 2 week irradiation (McIntyre, 2003). It was also noted that this system had a relatively low efficiency in that 3 times as much radioxenon activity should have been created during this irradiation period (McIntyre, 2003).

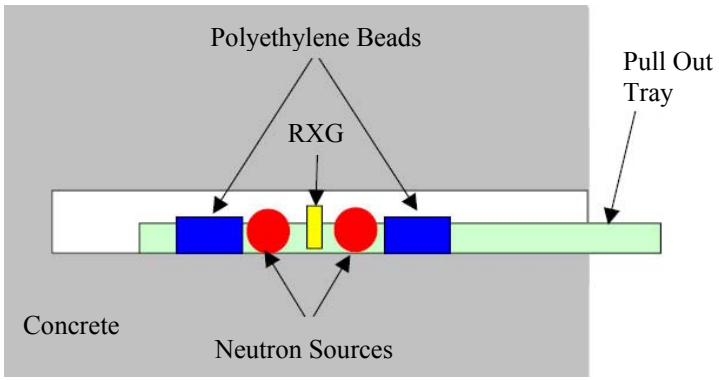

Figure 1) Configuration of the *radioxenon generator* (RXG) (McIntyre, 2003).

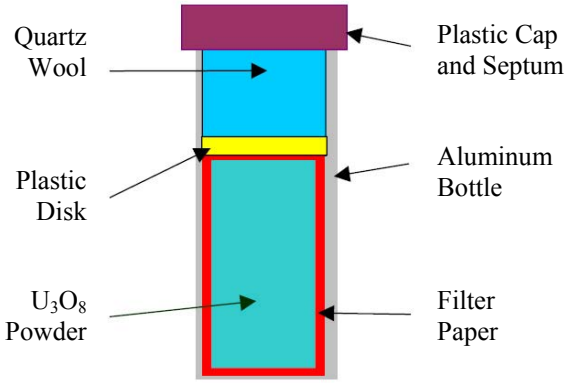

Figure 2) Schematic of the PNNL radioxenon generator (McIntyre, 2003)

2.4. RADIOXENON PHOSWICH DETECTOR DESIGN

The goal of this work is to generate fission-product xenon radioisotopes to demonstrate the proper operation of the XEPHWICH prototype. The XEPHWICH detector is a multi-layered scintillator type detector and has been developed at

Oregon State University to meet the goal of detecting the design limit of 1.0 mBq/m^3. An ideal scintillator has many important characteristics such as being transparent to its own light, possessing fast light emission times, a high degree of scintillation efficiency, light properties that are linear based upon the energy deposited into the detector, and overall good optical qualities (Knoll, 2000a). There are three main types of scintillating detectors; plastic, organic and inorganic scintillators. There exist several physical and chemical states for each detector type. Organic scintillators can exist as polymers, liquids, loaded scintillators, thin films and crystals. The inorganics are represented as crystals (e.g., NaI, CsI, CsF, CaF_2, ZnS, and LiI). The fluorescence of organic scintillators occurs from energy-level transitions within a single molecule, while the inorganic scintillators fluoresce when an excitation and de-excitation occurs within the lattice structure.

The newly designed detector uses several scintillating detector layers sandwiched together, referred to as a phoswich. The specific detector system that has been created at Oregon State University for radioxenon detection is referred to as a *radioxenon multi-layer phoswich detector* (XEPHWICH). An important characteristic of the combined detectors is that they are optically coupled in such a fashion that no light is lost and the efficiency is not compromised. Scintillators in the detector design are chosen in such a way that the response time of each material is varied enough such that it can be determined in which material an interaction occurred.

The designed XEPHWICH detector actually employs three layers of scintillators to achieve high counting efficiency in a beta and gamma radiation field. The first layer of the detector is designed to isolate and detect beta particles, and is made from a plastic scintillator material referred to as BC-400. The second layer of the XEPHWICH is utilized for the detection of the 30 keV x-ray photon that is emitted as part of the xenon decay, and is made from a thin organic scintillating crystal of CaF_2(Eu). The thin first two layers minimize the likelihood that incident higher energy photons will be stopped prior to reaching the third layer. The third layer, design specifically for the detection of gamma photons, is an inorganic scintillator and is made of NaI(Tl). Between the second and third layers rests a quartz crystal that allows for the NaI(Tl) scintillator to be hermetically sealed while, not significantly compromising light collection efficiency of the first two layers. **Figure 3** shows a schematic of the XEPHWICH detector. The specific material properties are located in **Table 1**, which includes the thickness of each layer.

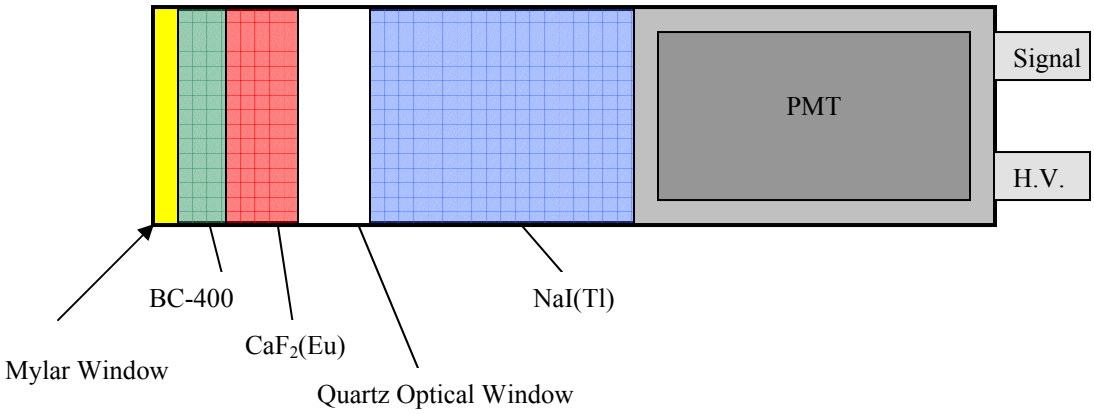

Figure 3) XEPHWICH detector schematic

Table 1) XEPHWICH material thicknesses and properties

Material	Thickness (inches)	Sensitivity
BC-400	0.06	Beta
$CaF_2(Eu)$	0.079	30 keV X-ray
NaI(Tl)	1.0	High Energy Photon
Quartz	0.25	Transparent

By using these specific materials together, and utilizing a digital pulse shape discrimination, both beta and gamma-ray energy distributions can be captured. This allows the device to determine if specific bombarding radiation is due to the characteristic xenon isotopes. The detector specifically allows for coincidence counting of beta-gamma radiation. This is vital because both xenon-133 and xenon-135 emit triple coincidence radiation in the form of beta, gamma and x-rays.

The completed XEPHWICH system will employ two identical detectors facing each other to increase the solid angle geometry. The xenon gas will be

injected into the volume between the detectors so that any radiation will most likely be deposited into one of the two detectors. The final assembled design of the detector will appear similar to the diagram in **Figure 4**.

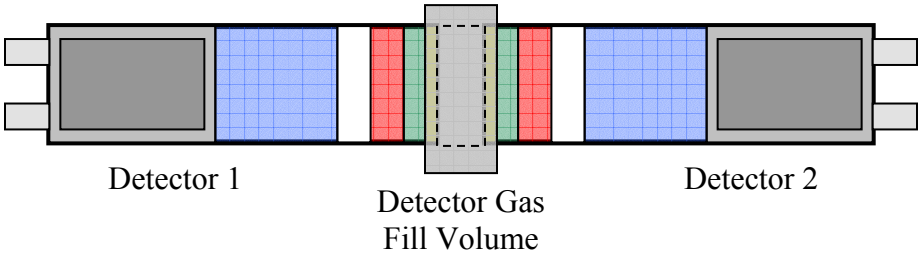

Figure 4) XEPHWICH Detector System

2.5. XENON APPLICATION IN MEDICINE

There currently is a use for some specific isotopes of xenon in the medical community that is somewhat relevant to this work. Xenon-133 is used for diagnostic purposes to evaluate pulmonary function and enable imaging of the lungs (Daily Med, 2003). It can also be used for enhanced tomography of cerebral blood-flow measurements (American Elements, 2008). Xenon is easily administered to patients by simple inhalation from a respirator system.

Several vendors sell xenon-133 in activities of 10 and 20 mCi (Covidien, 2008). The sample sizes are sold in 2.0 cm^3 vials that contain xenon and atmospheric air. The xenon samples are reactor produced as a fission product of uranium-235, however no filtering of byproducts is mentioned (Daily Med, 2003).

The prices for the samples described above are undisclosed, and further contact with a vendor would be necessary to determine cost and availability.

3. BACKGROUND

3.1. ISOTOPES

Each atom is made of three fundamental particles; neutrons, protons and electrons. The nucleus of an atom determines in which elemental state it will reside. The atomic nucleus is comprised of positively charged protons and neutrally charged neutrons. All atoms with the same number of protons, but a different number of neutrons, are considered to be the same element, yet different isotopes of that element. An example of hydrogen isotopes are that of hydrogen-1, hydrogen-2 and hydrogen-3 and are depicted in **Figure 5**. All hydrogen isotopes have only one proton, but hydrogen-2 and hydrogen-3 have one and two neutrons, respectively.

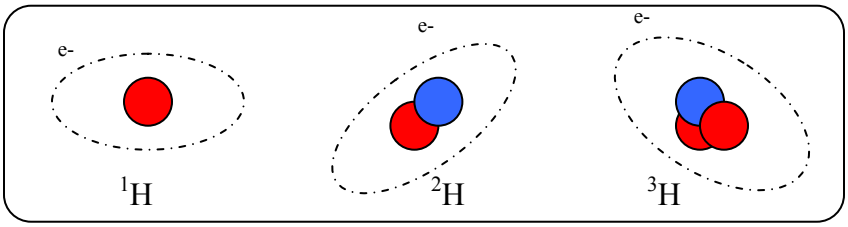

Figure 5) Hydrogen isotopes with protons and neutrons depicted.

The majority of the references to isotopes will be to those of xenon, in particular xenon-131, xenon-133 and xenon-135. It is important to mention that due to their similar chemical properties, isotopes of the same element are extremely hard to separate from each other (Lilley, 2001a).

3.2. FISSION

Fission is described as the physical process of splitting an atom into two smaller fragments. Certain nuclides, known as fissile nuclei, will more readily undergo the fission process when bombarded with a source of thermal neutrons (Lilley, 2001b). During the fission process, a neutron impacts the fissile atom nucleus and is captured. This new nucleus is referred to as the compound nucleus, denoted with a (*) symbol, and has a lifetime of approximately 10^{-16} to 10^{-18} seconds (Lilley, 2001c). The energy/mass imparted to the nucleus creates an unstable nuclear configuration and the atom subsequently divides into two individual pieces. This process is depicted in **Figure 6** and by the equation below.

$$^{235}U + {}^{1}n \rightarrow {}^{236}U^{*} \rightarrow {}^{99}Sr + {}^{135}Xe + 2n + \beta + \gamma + \upsilon$$

The two fission fragments are accompanied by the emission of several neutrons as well as prompt energetic gamma rays, beta particles and neutrinos.

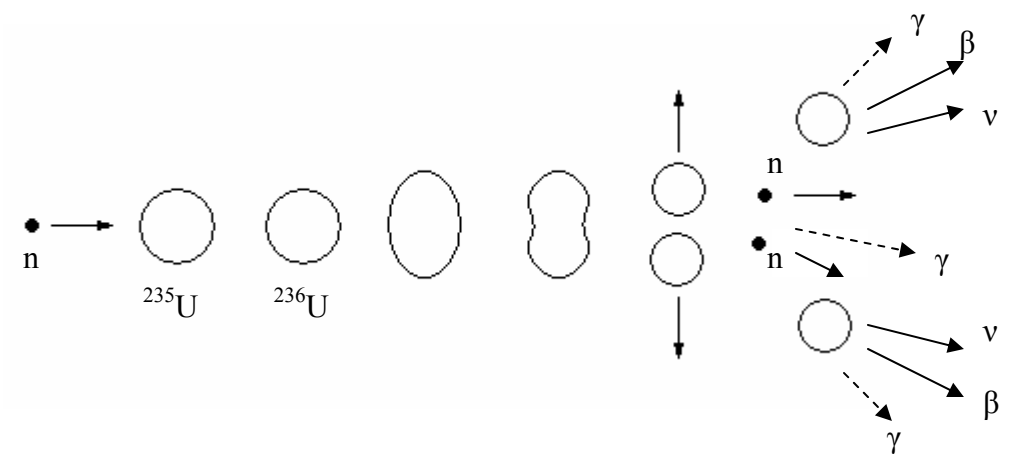

Figure 6) Fission process due to neutron bombardment[2].

Prompt and delayed gamma and beta emissions will be discussed further in the following sections, however a discussion on prompt neutrinos will be omitted as it has little to no importance to the scope of this work.

The relationship in **Figure 7** represents the probability that a fission event will result in the creation of a particular atom. The double-hump shape of the curve is particular to the fact that the two fission fragments are rarely of equal size. It also happens that the peak on the rightmost curve occurs at a mass number of approximately 135, and is represented by the production of xenon.

[2] Extracted from text, Figure 10.1 (Lilley, , 2001f)

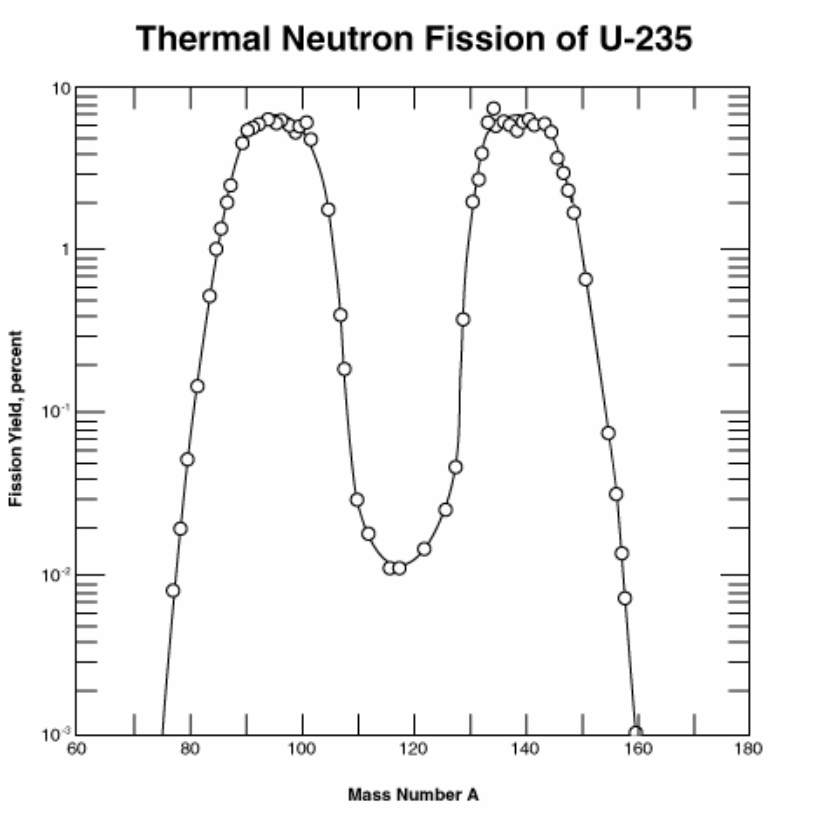

Figure 7) Distribution of fission fragments from fissioning uranium-235.[3]

3.3. EXPOSURE

The following subsections cover the necessary information that relates to the understanding and calculation of such quantities as dose, ALI and DAC. These calculations were necessary in determining the amount of radiation that would be presented to any individual exposed following the production of fission-product nuclides. These findings were vital in obtaining the approval of the

[3] Image pulled from http://www.science.uwaterloo.ca/~cchieh/cact/nuctek/fissionyield.html

experiment from the *Reactor Operations Committee* (ROC) at Oregon State University.

Exposure is defined in terms of the charge created by ionizations from secondary electrons within a given volume of air and a specific mass (Knoll, 2000b). This fundamentally equates to the amount of energy from x-rays or gamma rays that is imparted into a specific mass area. The historical unit of measurement for exposure is the *Roentgen* (R), and has a numerical value of

$$1\,\mathrm{R} = 2.58 \times 10^{-4}\ C/kg$$

The current SI unit of gamma-ray exposure is the (C / kg), and has not been given a specific name (Knoll, 2000b).

3.3.1. ABSORBED DOSE

The energy absorbed in the mass of any material from an incident radiation source is referred to as *absorbed dose.* The amount of energy absorbed by the material per unit mass from the radiation is highly dependent on the material type, thus two different materials will receive different absorbed doses from the same radiation source (Knoll, 2000b). Dose is normally measured using the current SI unit of 1 joule/kilogram or 1 *Gray* (Gy). It can also be measured using the historical unit of the *rad*, where:

$$1\,rad = 0.01\ Gy$$

Members of the general public, as well as individuals employed in the nuclear workforce must adhere to specific limits of dose set forth by governing agencies. These limits help the appropriate governing agencies regulate and monitor nuclear activities across the country. The dose limits are measured as a *total effective dose equivalent* (TEDE) to an individual. The effective dose equivalent utilizes weighting factors for specific organs and different radiation energy ranges to calculate the effective dose to an individual that may become exposed. Weighting factors for different radiations, W_R, are listed for a variety of incident radiation particles and energy ranges. Values for W_R vary from 1 to 20. The weighting factors for different organs, W_T, covers all major organs and varies with values from 0.01 up to 0.20. Effective dose is measured using the US units of rem, or the SI unit is currently the *Sievert* (Sv) where

$$1\,rem = 0.01\ Sv$$

The Nuclear Regulatory Commission limits the dose to any member of the public from a nuclear operator to 100 mrem per year[4]. A radiation worker however, may receive an occupational dose of 5,000 mrem per year from the same source[5].

To calculate dose, several important values must be known including:

- Flux
- Energy of flux
- Material properties for the absorbing material

---

4 From 10 CFR 20.1301 - Dose limits for individual members of the public

[5] From 10 CFR 20.1201 – Occupational dose limits for adults

- Duration of bombardment

With these values defined, the solution to a typical dose equation can be found. The following equation will be employed to calculate the external dose to an individual received from photons emitted by activated or fission-product sources.

$$D_\gamma = \phi_{Al}\left[\frac{\gamma}{cm^2 - \sec}\right]\cdot\left(\frac{\mu_{en}}{\rho}\right)_{tissue}\left[\frac{cm^2}{g}\right]\cdot E_\gamma[\mathrm{MeV}]\cdot 1.6\mathrm{x}10^{-10}\left[\frac{J\text{ - }g}{MeV\text{ - }kg}\right]\cdot t[\sec]$$

3.3.2. ALI

When radioactive material is dispersed into water or air, the mechanism through which it enters the body is most likely to occur by either inhalation or ingestion. The limits restricting uptake through these modes are calculated and based upon the *annual limits of intake* (ALI), and are based upon a reference individual of assigned anatomic, physiological and biochemical parameters (Cember, 1996a). The ALI is vital in calculating doses that may occur to individuals exposed to radionuclide dispersals over extended periods of time. The *International Commission on Radiological Protection* (ICRP) recommended the restriction of uptake based on a 50-year dose commitment, also referred to as an effective committed dose equivalent, not to exceed 5 rem.

3.3.3. DAC

The ALI as described previously helps to determine the allowable uptake for any individual based on specific criteria such as nuclides of interest. The ALI however only determines the maximum permissible amount of nuclide uptake, and not the direct mode of uptake. To appropriately calculate the duration an individual can be exposed before they exceed their maximum permissible dose as determined by the ALI, the rate of uptake by inhalation must be calculated (Cember, 1996b). Using the *derived air concentration* (DAC), the amount of uptake from inhalation over a period of time can be determined. For the DAC calculations it is assumed that an individual is exposed to airborne contamination for a 2000-hour working year with an inhalation rate of 20 L of air per minute. This equates to inhalation of 2400 m³ of air over the duration of the working year. The DAC is then calculated using the following method, producing a concentration of activity per volume.

$$DAC\left[\frac{Bq}{m^3}\right] = \frac{ALI\left[\frac{Bq}{year}\right]}{2400\left[\frac{m^3}{year}\right]}$$

The DAC was used to calculate the maximum concentration of activity that could be present in both the *Neutron Radiography Facility* (NRF), as well as the Reactor Bay to remain within the required limits.

3.4. FLUX

Flux is described as the number of particles per unit time passing through a given area. The flux term is designated using the Greek letter *phi* (ϕ). The common measurement of flux is described in units of

$$\phi\left[{particles}/{cm^2 \cdot \sec} \right]$$

where the definition of the particles is particular to each radiation type. Neutron flux is likewise defined as the number of neutrons passing though an area (cm^2) per second. A depiction of flux can be seen in **Figure 8**, showing the movement of some quantity across a surface.

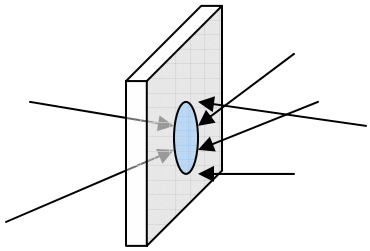

Figure 8) Depiction of flux

For neutron flux, the system can be more thoroughly described as fast, thermal or epithermal. These describe the energy level of the projectile neutrons; with fast neutrons represent higher energy neutrons, thermal[6] representing low energy neutrons, and epithermal describing the neutrons in the intermediate

[6] A thermal neutron corresponds to a neutron having energy of 0.0253 eV, which corresponds to a velocity of 2200 m/sec.

between the two. One way of defining the energy ranges for the three states of neutrons are displayed in **Table 2.**

Table 2) Neutron energy ranges[7]

Neutron Classification	Energy Range
Fast	>100 keV
Epithermal	1 eV < x < 100 keV
Thermal	<1 eV

The thermal flux of neutrons is the primary cause for the fission of the uranium-235 nuclide, and is therefore the greatest concern for the work encompassed by this thesis. Fission can also occur from fast and epithermal neutrons, but the highest fraction of fission events will result from the thermal flux concentration.

The region existing between the fast and thermal ranges, corresponding to the epithermal neutron energy range, is called the resonance region with respect to cross sections.

[7] The fast energy range is for neutrons above 100 keV (Cember, 1996c). However depending on reference, the energy range of the fast energy group may vary as much as four orders of magnitude.

3.5. NEUTRON INTERACTIONS

When neutrons impinge on a material, there are a variety of different interactions that may occur. The interaction type depends highly on properties of the target material, as well as other outside factors such as neutron energy.

3.5.1. CROSS SECTION

The cross section, or probability of a neutron interaction in a given material, varies widely, and spans several orders of magnitude depending on the type of interaction. Cross sections are expressed using the units of *barns* (b), and are depicted by the Greek symbol *sigma* (σ).The barn is used for the measurement of area, and is represented as

$$1\ barn = 10^{-24}\ cm^2$$

thus, hitting the broad side of 1 barn, is actually more difficult than it may seem.

For ease of use, cross sections are most often tabulated at 0.0253 eV, corresponding to the thermal neutron energy range for an incident neutron (Murray, 2001). For particular nuclides, such as boron-10 and uranium-238, cross sections are also tabulated in the fast and epithermal range due to their relevance in nuclear fission. If all of the interaction cross section mechanisms are combined, a *total cross section* (σ_t) can be calculated (Duderstadt, 1976a). The two main types of neutron interactions are scattering and absorption.

3.5.2. NEUTRON SCATTER

In neutron scattering, an incident neutron appears to deflect in the presence of a target atom, imparting a portion of the neutron energy to the atom. The total scattering cross section for a material is dependent on both the elastic and inelastic scattering cross sections. The total scattering cross section is simply,

$$\sigma_s = \sigma_e + \sigma_{in},$$

where σ_e and σ_{in} represent elastic and inelastic scattering cross sections, respectively (Duderstadt, 1976a).

3.5.2.1. ELASTIC NEUTRON SCATTERING

Elastic scattering (σ_e) describes the process of the collisions of an incoming particle and the target atom and is depicted in **Figure 9**. The energy imparted to the target atom is a direct function of the masses of the two particles and the scatter angle, as kinetic energy is conserved in this scattering mechanism. This also results in conservation of momentum, so that the resulting energy can be determined if the incoming energy, scattering angles and the particle masses are known (Knoll, 2000c). Thus, with elastic scatter the target atom gains kinetic energy and its excitation energy remains in the ground state.[8]

[8] Ground state of an atom implies that the nucleus of the atom does not contain excess energy and thus does not need to emit energy through radiative processes.

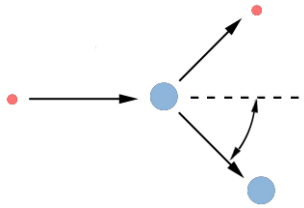

Figure 9) Elastic neutron scattering

3.5.2.2. INELASTIC NEUTRON SCATTER

The key difference between elastic and inelastic scattering is the energy imparted on the target nucleus. In inelastic scattering, the target nucleus is left with excess energy in an excited state. This energy absorption means that momentum was not conserved, and some of the kinetic energy that was deposited into the compound nucleus was retained as excitation energy.

3.5.2.3. NEUTRON MODERATION

Neutron moderation describes the process of multiple scatterings in which a neutron loses energy each time it interacts with a target nucleus. This loss in energy of the neutron is considered moderation, because it allows the neutron to impart its kinetic energy into the surrounding material so that the neutron slows down. Moderation is a function of the material mass, the neutron mass and the neutron velocity. The effectiveness of a moderator is relative to the material's atomic mass. The scattering method between the target nucleus and the incoming neutron means that the most effective moderator will have an atomic mass similar

to that of the neutron. A neutron's atomic mass is essentially 1 *atomic mass unit* (amu), meaning that the best neutron moderator will also have an atomic mass of 1 amu, such as hydrogen. All materials can be used as a neutron moderator, but their effectiveness to slow the neutron depends on the material scattering cross section as well as the atomic mass. Take, for example, the comparison between carbon-12 and hydrogen-1 as a moderator. For hydrogen-1, 18 interactions are required to slow a neutron from fast to thermal energy, while for carbon-12, 115 interactions are required (Lilley, 2001d).

3.5.3. NEUTRON ABSORPTION

Absorption is the process where an incident neutron is absorbed into the nucleus of the target material. The ability of a material to be an effective neutron absorber depends heavily on the relative magnitudes of the absorption and scattering cross section of that nuclide. If a nuclide has a much greater neutron absorption cross section compared to the neutron scatter cross section, incident neutrons will be more likely to be absorbed than scattered (Lilley, 2001d). Absorption can be considered as a type of fusion, as it allows for the target nucleus to increase in mass, although this nucleus may be unstable and decay. The new nucleus may either release excess energy through neutron capture, resulting in the emission of gamma rays, charged particles or neutrons, or it may split into

several pieces through fission. The total absorption cross section is the sum of both the capture and fission cross sections, and can be denoted as the following:

$$\sigma_a = \sigma_c + \sigma_f$$ [9]

Considered a strong neutron absorber, boron-10 is often used to control the fission process in a nuclear reactor by capturing excess neutrons. Although this nuclide does have a relatively large cross section, 3.84 x10³ b, it is still several orders of magnitude less than that of the xenon-135 isotope (2.65 x 10^6 b), which is considered a neutron "poison" in nuclear reactors due to the ability of the nuclide to "steal" neutrons from the fissioning process. In the context of a nuclear reactor, xenon is an undesirable byproduct created during the fission process.

3.5.4. NEUTRON FISSION

Fission is the process in which the nucleus of an atom becomes unstable and splits into two separate pieces, referred to as fission products, accompanied by the emission of neutrons and electrons. The number of neutrons and electrons emitted due to fission depends on the nuclide that is being fissioned, but generally involves a few neutrons and electrons per fission. The fission cross sections for many fissile nuclides are well documented and cataloged. These cross sections often vary over several orders of magnitude depending on the incident neutron energy. **Figure 10** shows the neutron fission cross section for the uranium-235

[9] The absorption cross section is also defined as $\sigma_a = \sigma_t - \sigma_s$, or as the summation of all non scattering cross sections (Duderstadt, 1976a).

nuclide. From this figure it is easy to discern the resonance region of the cross section, which is apparent by the sharply oscillating center of the graph. The thermal and fast regions are smoother than the epithermal region, and are located on the left and right of the graph respectively.

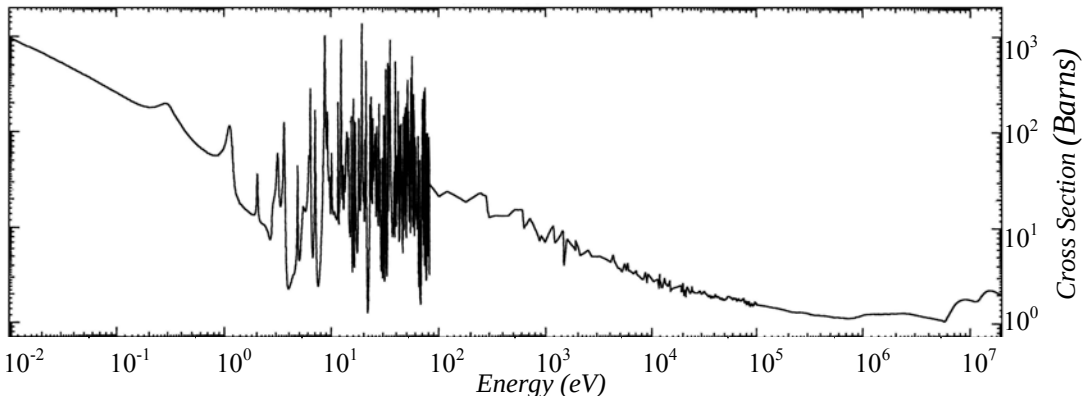

Figure 10) Neutron fission cross section for uranium-235[10]

3.5.5. CAPTURE

As discussed earlier, the total absorption cross section is the sum of the fission and the capture cross sections. Neutron capture is characterized by a neutron being absorbed into the nucleus of an atom, and not resulting in fission. In non-fissionable nuclides, the capture and absorption cross section are one and the same. There are several outcomes that occur when a nucleus captures a neutron. The first scenario is that the absorption of the neutron will result in a stable isotope of the same element. An example of this is the capture of a neutron by

[10] Figure 2-17 taken from text (Duderstadt, 1976b)

carbon-12 to result in carbon-13. The carbon-13 isotope is a stable nucleus and no further decay will occur. The alternative scenario is where the neutron is captured, resulting in an unstable nucleus. As defined previously, this unstable nucleus will not cause fission; rather it will lead to a decay mechanism in which the nucleus releases the excess energy that was imparted to it when it captured the neutron.

3.6. MODES OF DECAY

The process of releasing excess energy from an excited nucleus is achieved though the emission of excess mass or energy through several different decay modes. The mode of decay is dependent on several factors, such as the specific nucleus of concern, and how much energy must be released to achieve stability. The prominent decay modes are alpha emission, beta-minus decay, *positron* (beta-plus) decay and electron capture, where electron capture is a competing with positron emission. The mode of decay is generally dependent upon where the nuclide rests on the Chart of the Nuclides. As seen in **Figure 11**, the highlighted sections correspond to the prominent modes of decay. In the red highlighted area, alpha emission is the driving decay mechanism. The blue area corresponds to beta-minus decay, leaving the green section for the competing positron and electron capture decay mechanisms. These four modes of decay will be briefly described in the following section.

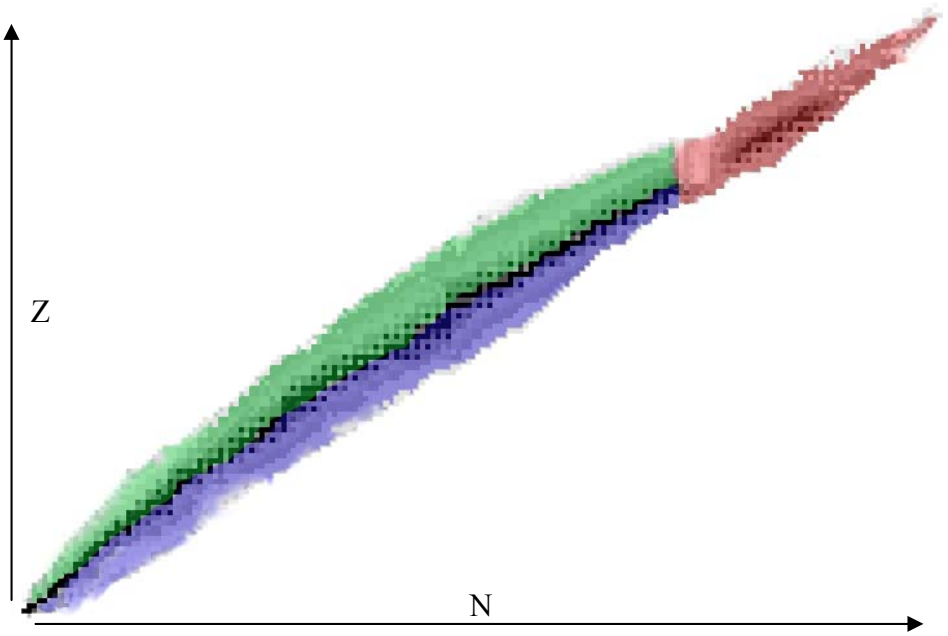

Figure 11) Chart of nuclides highlighting driving decay modes

3.6.1. ALPHA

Alpha (α) emission referrers to the ejection of an alpha particle from the nucleus of an atom, and occurs in heavy atomic nuclei. An alpha particle is essentially the nucleus of the helium-4 atom. This alpha particle, which contains two protons and two neutrons, is the heaviest of the prominent decay modes, which allows for the emission of large quantities of energy. Decay energies from alpha emission are often in the MeV range, which if deposited internally in a living organism can be devastating. Many naturally occurring elements such as uranium, radon, radium and thorium decay by alpha emission to move towards a steady state at lead (Pb). Artificially produced transuranic elements also prominently decay by the alpha emission process.

One important characteristic that is observed through the alpha decay mechanism is the recoil nucleus effect. The nucleus of the decay atom has a mass on the same order of magnitude as that of the alpha particle, thus as the alpha particle is ejected, conservation of momentum causes the nucleus to recoil.

In the process of alpha emission, the energy released from the reaction is highly characterized and discrete. Most nuclides that have prominent alpha emission decay mechanisms have been recorded and are easily found in databases such as the Chart of the Nuclides and the National Nuclear Data Center.

3.6.2. BETA

Beta decay, signified by the β symbol, is a common source of energy release through the process of *electron* (e^-) or *positron* (e^+) emission. Although the nucleus of the remaining atom does recoil in a similar fashion as described from the alpha emission process, the recoil energy is minimal due to the minuscule mass of the beta particle recoiling particle, and is normally neglected. The process of decay by *beta-minus* (β^-), an electron, is only prominent in neutron rich nuclides. In this instance, the electron is ejected from the nucleus, resulting in a net increase in charge by one. This mechanism can be conceptually thought of as the transformation of a neutron into a proton and electron. In this decay mechanism, the nuclide boron-12 would decay to the stable carbon-12 isotope.

For *positron* (β^+) decay, the positron behaves similarly to a positively charged electron, with the identical mass. This positron decay mechanism occurs in proton rich nuclei, resulting in the decrease of the nuclear charge by one unit. Results of the decay process of both beta-minus and positron decay can be observed in **Figure 12** below. In this figure, the shaded nuclides represent stable nuclei, with the upper left nuclei proton rich, and the lower right nuclei neutron rich nuclides.

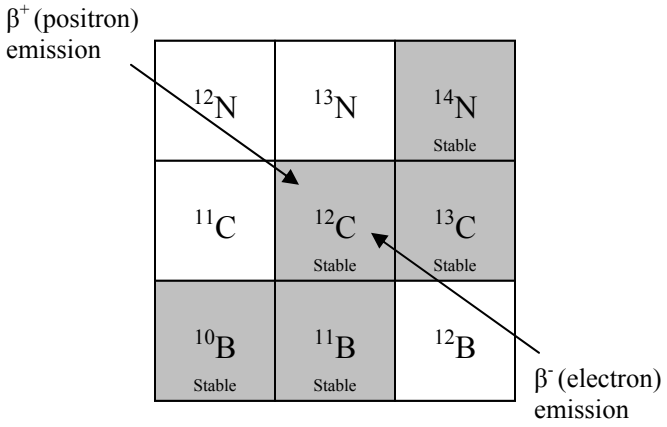

Figure 12) Beta decay emissions and resulting nuclides

Unlike alpha emission, the energy released from the beta emission process is continuous due to the presence of *neutrinos* (υ) and *anti-neutrinos* ($\overline{\upsilon}$). The anti-neutrino has no charge and no discernible rest mass, but shares the decay energy with the beta-minus emission process and helps to account for the loss in decay energy (Lilley, 2001e). The positron decay energy is likewise offset by the presence of neutrinos. Although certain energy releases are more prominent than

others, the probability of release at all encompassing energies does still exist and is apparent from the beta-minus energy spectrum (**Figure 13)**.

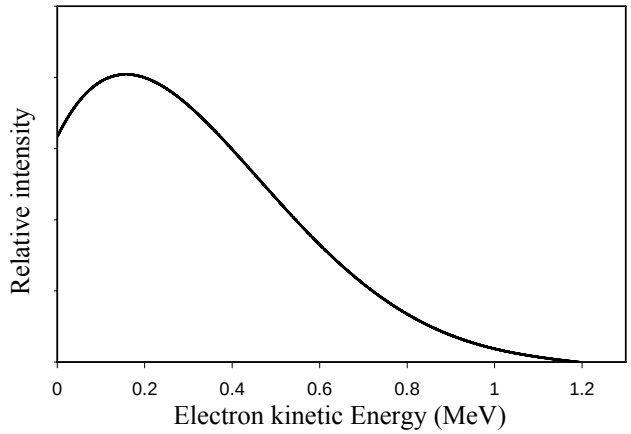

Figure 13) Energy spectrum of beta particles emitted from bismuth-210

This conceptually means that although a maximum of 1.2 MeV may be possible for the emitted beta emission, it is probable that the energy will be at some value between 1.2 MeV and zero, with a more probable value around 0.2 MeV. In most forums, when discussing the process of beta decay, the discussion is that of the beta-minus emission. In most other instances, β^+ is strictly referred to as positron decay.

3.6.3. ELECTRON CAPTURE

Electron capture, the mechanism competing with positron decay, occurs when an electron and proton are transformed into a neutron and neutrino. This mechanism can be expressed as:

$$p + e^{-} \rightarrow n + \upsilon$$

This occurs when an electron from the innermost orbital shell is pulled into the nucleus of the atom, resulting in the transformation. The newly created neutron remains in the nucleus, while the energetic neutrino is released as decay energy. Electrons from other orbital shells could cause this transformation, but it is less likely (Lilley, 2001e).

3.7. GAMMA EMISSION

Gamma (γ) emission refers to the ejection of an energetic photon with no mass. Gamma emission usually accompanies some other type of decay, such as beta emission. In this circumstance, a variety of gamma ray emission combinations can occur after the beta decay for the nucleus to reach a stable state. **Figure 14** depicts the mechanism of gamma emission to the ground state for cobalt-60 following beta decay.

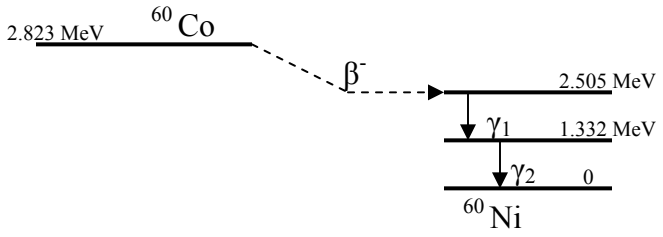

Figure 14) Decay scheme for cobalt-60

Cobalt-60 decays with a 0.318 MeV beta-minus emission, followed by two succeeding gamma emissions. The first gamma emission is 1.173 MeV, followed by a 1.332 MeV gamma photon occurring simultaneously. This allows the cobalt-60 to reach the stable nickel-60 state. Gamma emission is often referred to as a secondary decay mode that allows the compound nucleus to release excess decay energy. These well-characterized emissions occur at discrete energies and have been tabulated for most nuclides.

3.8. METASTABLE STATES

Through the process of decay, a nuclide that retains its excitation energy for an appreciable length of time (>1 sec) is said to be in a metastable state. This metastable state is a temporary or intermediate condition of the nucleus as part of the process for the atom to reach the ground/stable configuration. The metastable state is denoted as a superscript (m), demonstrated here in the metastable xenon-133 isotope:

$$^{133m}Xe$$

Isomeric Transition (IT) refers to the transition from the metastable to the stable state, and is signified by the first gamma ray emission in that transition. Thus, an IT is simply the first gamma-ray emitted from a metastable nuclide releasing energy on its path to becoming stable. Subsequent photon emissions are simply called gamma emissions.

3.9. SPONTANEOUS FISSION

In rare occurrences, certain very heavy nuclides will decay spontaneously through the spontaneous fission process. Spontaneous fission is similar to the process of neutron-induced fission, with the exception that no additional incident energy is necessary to cause the process. For those nuclides that can fission spontaneously, the nucleus is naturally in an excited unstable configuration and is in need of releasing this extra energy. Most often, this energy will be released through alpha decay or beta emission, but in some circumstances spontaneous fission is possible. One prominent spontaneously fissioning nuclide is californium-252. Although californium-252 does fission spontaneously, it still has a higher probability of alpha emission as a means of radioactive decay (Knoll, 2000d).

3.10. ATTENUATION

Attenuation is the process of reducing the flux of neutrons or photons through a given medium. Attenuation is illustrated by the change in beam intensity before and after that beam traverses a given material. The equation for describing attenuation is given as the following:

$$I = I_o e^{(-\Sigma x)}$$

where Σ is the macroscopic total cross section, x is the material thickness, I_o is the initial beam intensity, and I is the final beam intensity. The macroscopic cross

section is material and energy dependent, and can vary widely depending on the medium of travel.

The attenuation calculation is vital in determining the intensity of a neutron beam that has penetrated a material. This will be used in a subsequent section to determine the relative intensity of the neutron beam after it has passed through the irradiation chamber of our fission device.

3.11. ACTIVATION

Certain nuclides, when bombarded with neutrons, have the affinity to absorb these neutrons and become a different atom. The neutron absorption cross section describes the ability of this nuclide to absorb a neutron. Take, for example, the widely used material aluminum-27, with a neutron absorption cross section of 0.23 barns. When aluminum-27 absorbs a neutron, it is *activated,* and becomes aluminum-28, which decays through beta emission. Activation is strictly used in describing the process of bombarding a material with neutrons such that the material does not fission, but rather it transforms to an atom with an additional neutron, and subsequently decays. Some materials may be bombarded with neutrons without becoming activated. Such materials are carbon-12 and hydrogen-1 which become the stable carbon-13 and hydrogen-2 isotopes, respectively.

One notable process of activation is the creation of gold. Gold can actually be created by activating stable platinum-196, which in turn becomes platinum-197. The platinum-197 then transforms to stable gold-197 by beta decay. Unfortunately, platinum is still more expensive than gold, so this application has no practical purpose.

Activation is also used in determining trace characteristics of materials. By bombarding a sample with neutrons and activating the materials, the decay energies from the activated trace elements can be detected. From these decays, the original material isotopic abundance of trace materials can be calculated. This process is useful in geological dating and forensic studies.

3.12. PROPERTIES OF FISSION PRODUCT GASES

During the fission process, a plethora of products are created with a wide range of properties. From the fission products produced, only two are created as noble gases, krypton and xenon[11]. Of these, xenon is more prominently produced during the fission process. Other nuclides such as cesium are decayed from xenon, so may temporarily be suspended as a gaseous product. This process will be discussed further under the *Decay Chain* section.

[11] As defined in the NRC glossary of fission gases (U.S. NRC, 2008)

3.13. PROPERTIES OF XENON

Xenon as it exists in the earth's atmosphere has a relative fractional abundance of approximately fifty parts per billion[12]. A member of the noble- or inert-gas category, xenon is not readily reactive with other compounds or elements since its outer electron shell is completely occupied. Xenon is also one of the heaviest noble gases, second only to radon. The major source of artificially obtained xenon is as a byproduct from the liquefaction and separation of air. This extracted xenon is used in a variety of applications, including fill gas for lights. As mentioned before, xenon and krypton are the only noble gas byproducts created as a result of the fission process.

As a colorless, odorless, tasteless gas, xenon is also non toxic. In nature, it exists as ten stable isotopes, but there also exists as many as 29 other unstable isotopes of the element. Of the radioactive isotopes, the longest lived is xenon-127, with a half-life of 36.4 days. **Figure 15** shows the relative position on the right side of the periodic table of elements where xenon resides as element 54.

[12] Los Alamos National Laboratory states that xenon exists at a concentration of about one part in twenty million in the atmosphere (LANL, 2008)

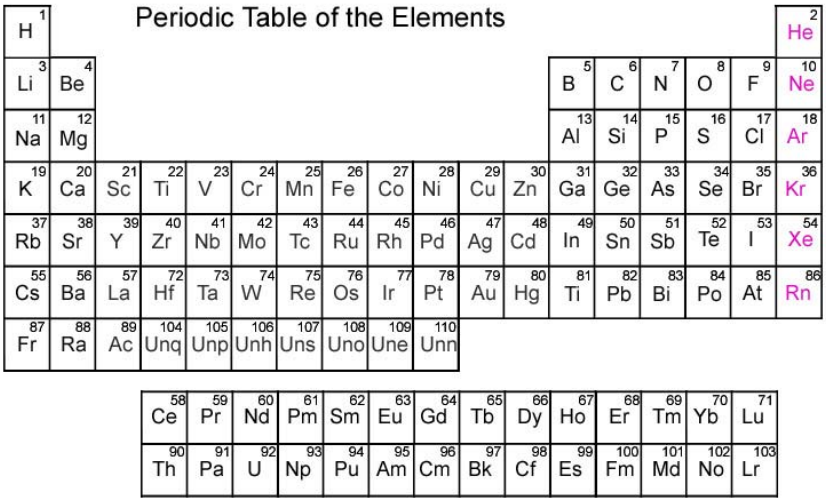

Figure 15) Periodic table of elements highlighting the noble gases[13]

As mentioned previously, the four specific xenon isotopes of interest are xenon-131m, xenon-133m, xenon-133 and xenon-135. Each of these nuclides has different decay energies which will make it distinguishable from the others. Table 3 shows the x-ray and gamma-ray energies that are emitted from the decaying xenon isotopes (ENSDF, 2007). The detection of these specific energies will identify each nuclide.

Table 3) Xenon isotope decay energies

Nuclide	X-ray [keV]	γ-ray [keV]
xenon-131m	29.62	163.93
xenon-133m	29.62	233.22
xenon-133	30.80	80.997
xenon-135	30.80	249.77

[13] Original image obtained from the Elements Database (Elements, 2008).

3.14. FISSION YIELD

Fission yield describes the byproduct elements created due to the fission process. As mentioned previously, the creation of any one nuclide is a probability and is therefore described as an independent fission yield for each nuclide.

A cumulative fission yield describes the fission yield of a specific nuclide taking into consideration all of the independent fission yields of nuclides that will decay into the nuclide of interest. Take, for example, the fission yield data for the simplistic decay chain

$$^{94}Br \rightarrow ^{94}Kr \rightarrow ^{94}Rb \rightarrow ^{94}Sr \rightarrow ^{94}Y \rightarrow ^{94}Zr\ .$$

The independent fission yield for the zirconium-94 is only 0.0195%. This means that only 0.0195% of the time will fission directly result in the creation of zirconium-94. However, other nuclides may be created during fission that then decay to create zirconium-94. If all of these other nuclide independent yields are accounted for, the cumulative yield for zirconium-94 can be found. **Table 4** shows the independent and cumulative fission yield data relating to the zirconium-94 nuclide.

Table 4) Independent and cumulative fission yield data for the 94 decay chain

Nuclide	Independent Yield	Cumulative Yield
Br-94	0.0002	0.0002
Kr-94	0.0868	0.087
Rb-94	1.5618	1.6488
Sr-94	4.4145	6.0633
Y-94	0.3899	6.4532
Zr-94	0.0195	6.4727

3.15. DECAY CHAIN SCHEME

As previously described, xenon is created as a byproduct of fission. The yield of xenon from the fission process is the cumulative of all of the independent yields of the nuclides that decay into the xenon isotope of concern. As an example of the process, an examination of the 133 decay chain is given in **Figure 16**.

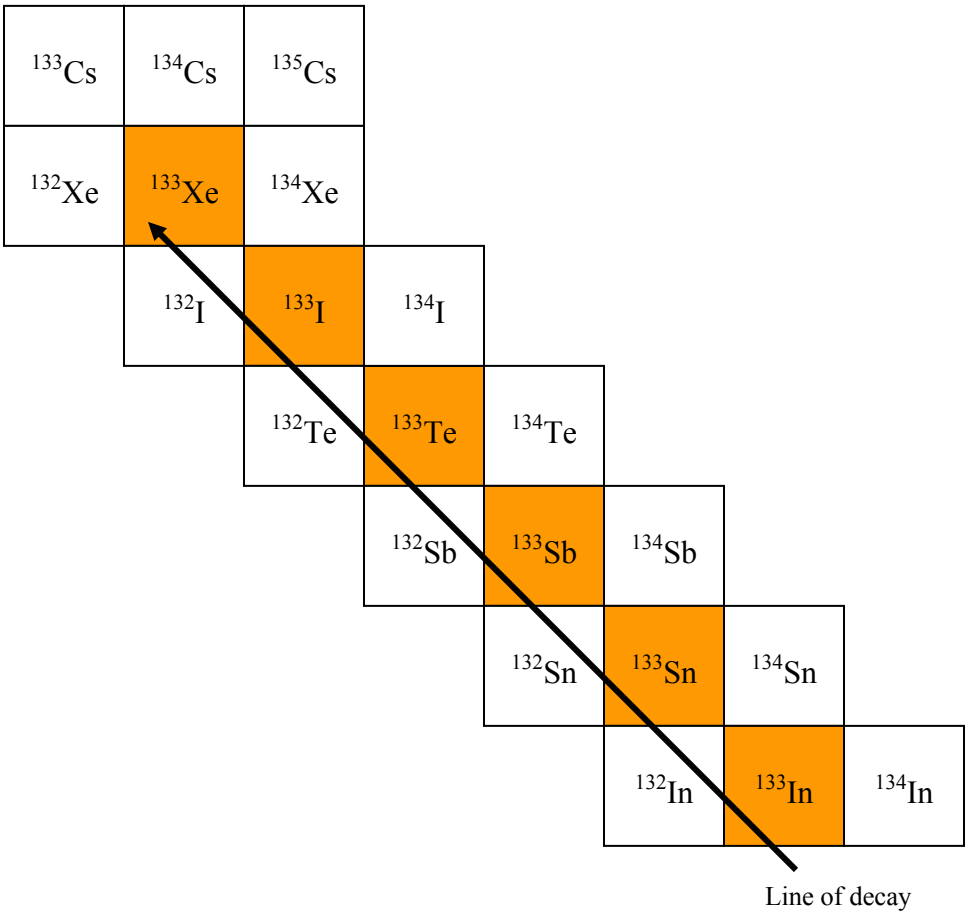

Figure 16) Decay line for the 133 decay chain

As observed in the figure, starting with indium-133 the isotopes decay by beta emission and work their way to the stable cesium-133 isotope. The

independent and cumulative yields for the 133 decay chain are listed in **Table 5** for the eight nuclides in the chain. The fission yield data are specific to the fissioning of uranium-235 by absorption of thermal neutrons. All of the nuclides in this decay chain will eventually decay to xenon, thus any nuclide created could eventually be available for detection from an underground nuclear detonation. Additional fission yields for other decay chains of interest are listed in **Appendix D**.

Table 5) Independent and cumulative yield values for the 133 decay chain[14]

133 Decay Chain			
Isotope	Half-life	Independent Yield	Cumulative Yield
In-133	0.18 sec	0.0002	0.0002
Sn-133	1.44 sec	0.1377	0.1379
Sb-133	2.5 min	2.2596	2.3975
Te-133m	55.4 min	2.9863	3.9932
Te-133	12.4 min	1.1482	3.0579
I-133	20.8 hr	0.1650	6.6970
Xe-133m	2.19 days	0.0019	0.1894
Xe-133	5.243 days	0.0007	6.6996
Cs-133	Stable	--	6.6996

[14] Data from LANL database on thermal neutron fission (England, 1993). Note that due to branching ratios that some of the cumulative yields seem misleading. **Appendix D** shows the branching ratio relationships for additional clarification.

4. DESIGN

A device was created to irradiate a *highly enriched uranium* (HEU) foil to obtain xenon fission gases. The two main components for this device are the gas supply system and the fission chamber. The fission chamber is where the HEU will be placed during irradiations. The gas supply system is the remainder of the device, which includes a series of valves, filters, piping and other components.

4.1. FISSION CHAMBER DESIGN

The major obstacle encountered in the design process was ensuring that the chamber could indeed hold a vacuum so that the fission gases would not be released accidentally. There are many ways to create a vacuum tight seal, but by far the easiest is by a flange design where two pieces of material may be mated together with an inlaying seal or o-ring.

4.1.1. ALUMINUM FLANGE

A flange design was chosen and constructed due to its simplicity and assurance that a vacuum seal could be obtained. The material for the chamber was chosen to be aluminum due to its neutron absorption characteristics. Aluminum is fairly neutron transparent, resulting in only a slight attenuation of the incident neutron beam.

Another important characteristic is the activation products created as a result of neutron exposure. For aluminum it is simply aluminum-28, since all naturally occurring aluminum is aluminum-27. Aluminum-28 has a relatively short half-life of only 2.25 minutes, which allows for fast decay of the activation products. This means that the sample can be handled shortly after irradiation, so the fission gas can be sampled whenever deemed necessary.

The design of the aluminum chamber itself was created around two requirements: the ability to hold a one square inch foil sample, and the ability to hold an O-ring. The O-ring dimension requirements are arbitrary since O-rings can be ordered in a variety of sizes. The foil sample dimension was chosen after discussing the potential sample size that would be used for the irradiation experiments. **Figure 17 – Figure 23** contain drawings of both flange pieces, referred to as simply the flange top and bottom. The drawings include a limited amount of dimensions, in inches, and views in this section. Detailed drawings can be found in **Appendix C,** and the Solid Works files are also available in **Appendix E.** The first set of drawings show the flange top, followed by the flange bottom and an assembled cut away view.

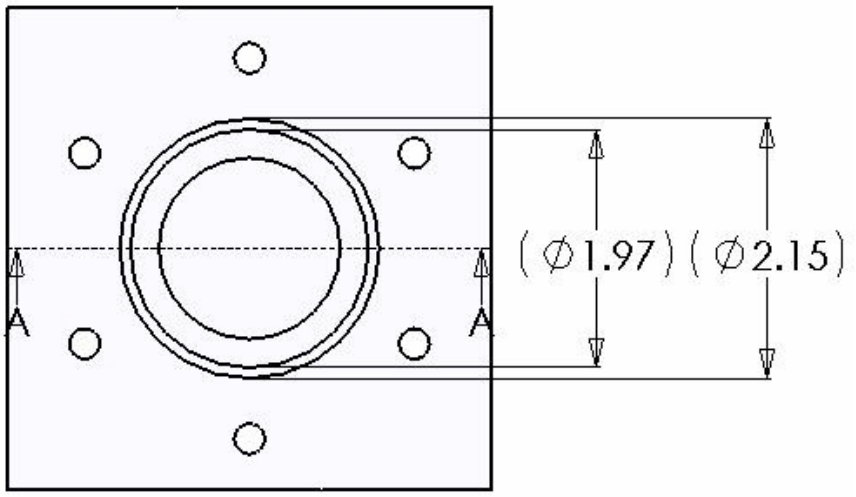

Figure 17) Top view of top aluminum flange

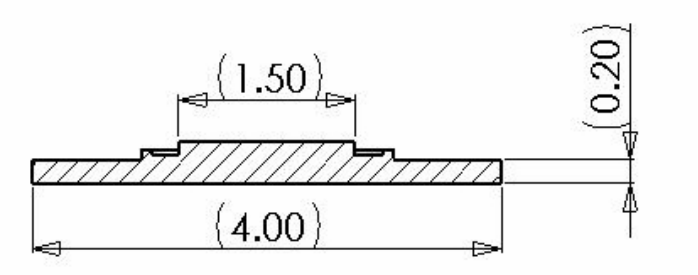

Figure 18) Cut-away side view of top aluminum flange

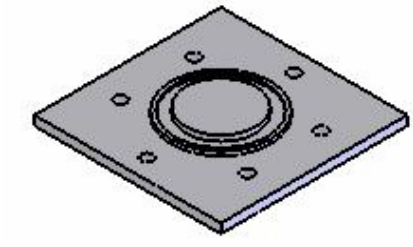

Figure 19) Isometric projection of top aluminum flange

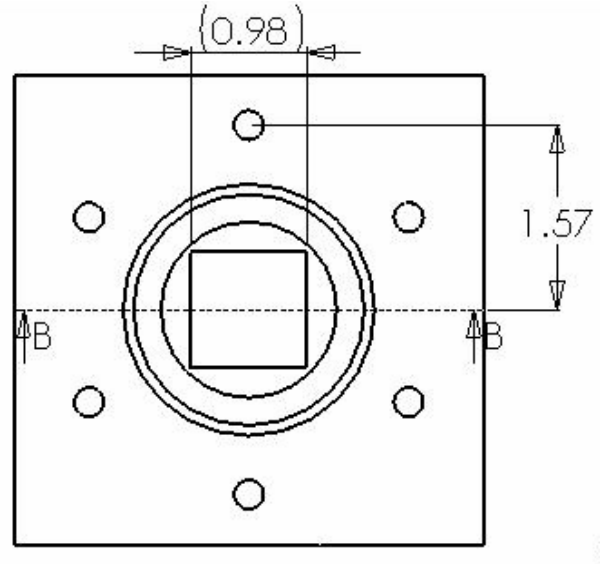

Figure 20) Top view of bottom aluminum flange

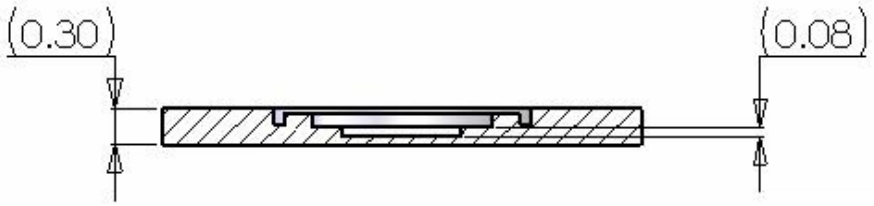

Figure 21) Cut-away side view of bottom aluminum flange

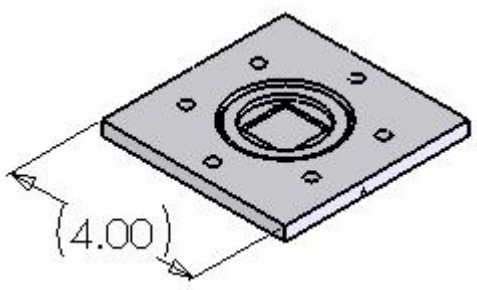

Figure 22) Isometric projection of bottom aluminum flange

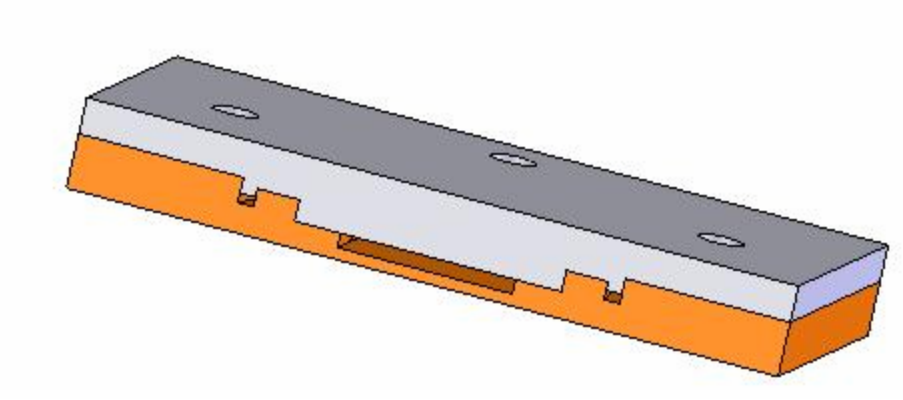

Figure 23) Cut-away view of flange assembly

The aluminum chamber was machined using the *Computerized Numerical Control* (CNC) machine located in the Radiation Center. The parts were milled to ensure that the tolerances would be sufficient to allow for the parts to mate effectively, while not reducing the tolerances such that the chamber would not be hermitically sealable. Several images (**Figure 24 - Figure 27**) were taken during the milling process. Due to some inconsistencies in the CNC machine, the surfaces of the chamber were not precisely level. This had no major impact on the manufacturing of the aluminum fission chamber, however, this flaw did cause the inlaying cut for the o-ring to not be precisely smooth, thus resulting in the accumulation of small metal burrs.

Figure 24) CNC milling machine head and aluminum sheet

Figure 25) CNC milling machine completing cut feature

Figure 26) CNC milling machine and manual controls

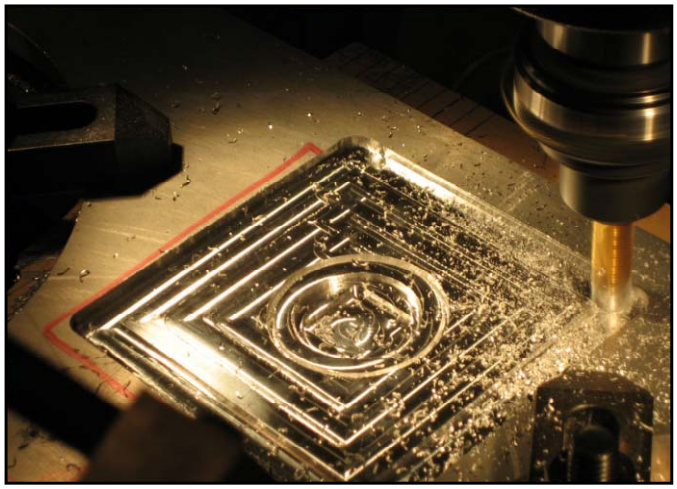

Figure 27) Milling of aluminum fission chamber

4.1.2. O-RING

As mentioned, an O-ring was used to seal the two aluminum chamber halves. Although a standard O-ring would have been sufficient, it was determined that an X-ring style would allow for the best seal due to the material surface roughness. The design of the X-ring, as seen in **Figure 28,** allows for the sealing of all four surfaces (inside diameter, outside diameter, top and bottom) with which the ring comes in contact. This equates to the higher probability of achieving the sufficient seal needed for this application. The o-rings are constructed from Standard Nitrile, also known as Buna-N, which are highly resistant to corrosion (Marco, 2007).

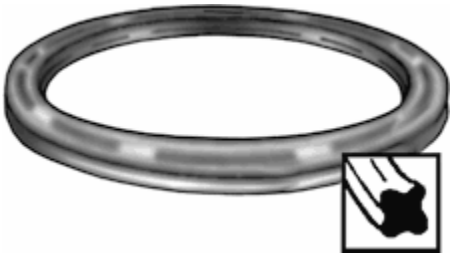

Figure 28) X-ring used to seal the aluminum flange halves[15]

4.2. DESIGN OF APPARATUS

The entire fission apparatus was designed with redundant safety, and the minimization of active volume in mind. The apparatus was designed so that the

[15] Image retrieved from McMaster-Carr (McMaster, 2008)

aluminum fission chamber could be replaced after the sample had undergone the maximum amount of irradiations. The system was also designed to be vacuum tight so that it would not leak fission products into the surrounding environment. Swagelok fittings were used for the connection of the parts of the gas supply system. The Swagelok-type fittings allow for a hermetic seal, while also allowing for many disconnection and reconnection options. One major advantage of the Swagelok fittings is that they do not require any type of sealing mechanism such as O-rings or pipe tape, due to their high tolerance manufacturing.

The overall design of the device utilizes a plethora of valves to assure that the fission gas only travels to desired locations. **Figure 29** shows the design of the complete fission apparatus and gas handling system. The tubing diameter varies from 0.025 inches to 0.0625 inches depending on location. The small diameter tubing is used to minimize the overall volume of open space near the fission chamber.

The components of the apparatus consist of either brass or stainless steel material, with the exception of the irradiation chamber which is made solely of aluminum. Aluminum is not necessary for the other gas supply system components, because they are not subjected to the highly collimated neutron beam.

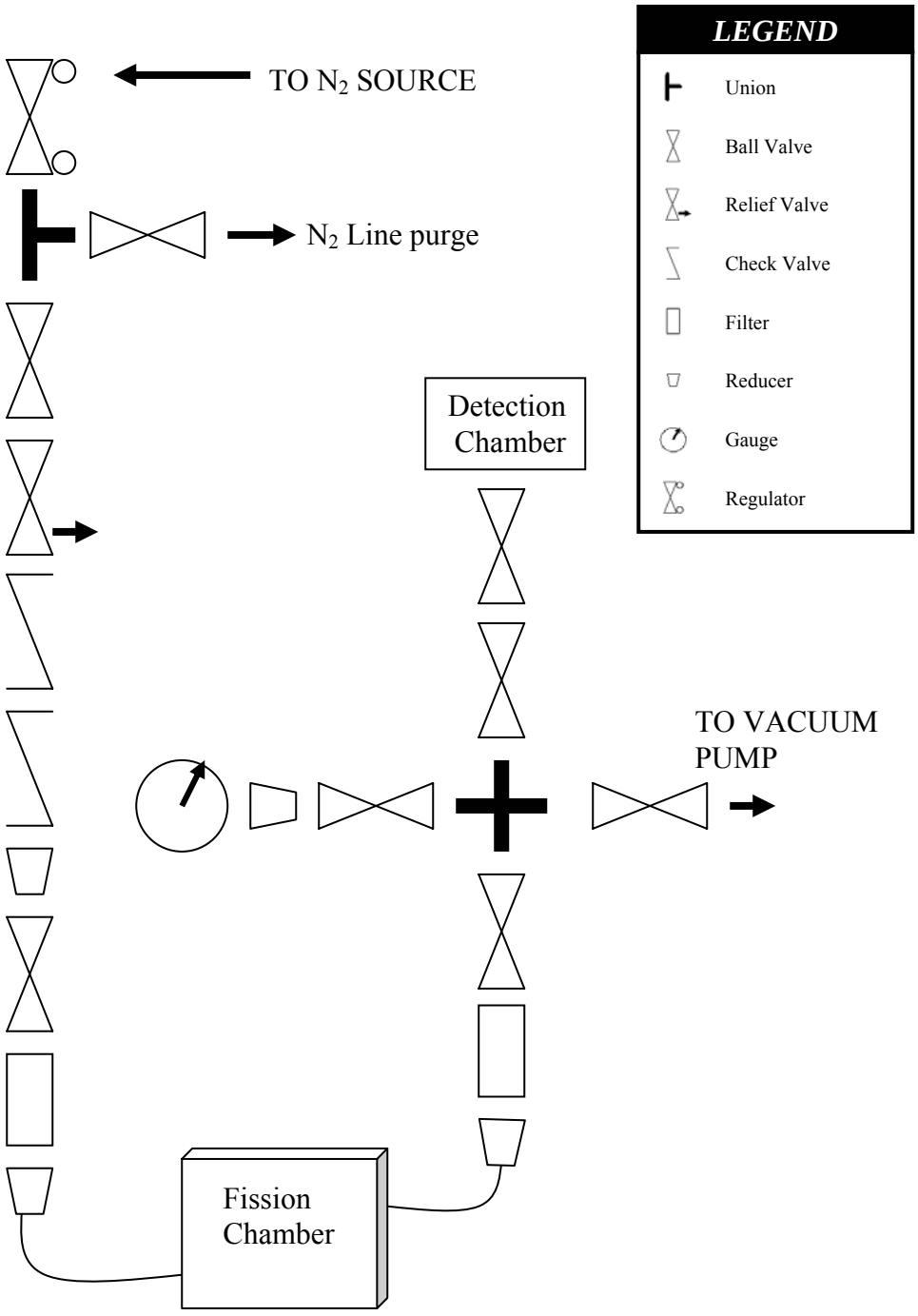

Figure 29) Complete fission apparatus and gas handling system design

4.2.1. DESCRIPTION OF VALVE TYPES

The variety of valve types utilized for the gas supply system allows for the diversity needed to meet the necessary specifications. The majority of the valves employed are simple ball valves that operate by turning a handle that is attached to a ball inside the valve structure. These valves are highly reliable, simple and provide a hermitic seal due to the O-ring located inside the valve. **Figure 30** is a cut-away view of a simple ball valve used in the apparatus.

Figure 30) Cut-away view of a Swagelok ball valve[16]

The second type of valve utilized is a check valve to ensure that no fission products travel upstream from the irradiation chamber. Check valves are essentially a small device that ensures the flow only occurs in the direction desired. It achieves this with an internal spring that releases the poppet once the upstream pressure has reached a certain value. For this application, a pressure of 1.0 psig is necessary to open the poppet. The apparatus created uses a double-check-valve design to provide a margin of safety ensuring that no fission products

[16] Image from Swagelok (Swagelok, 2008a)

travel upstream. **Figure 31** provides a cut away depiction of how a check valve operates.

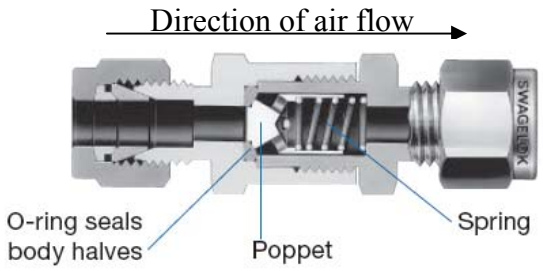

Figure 31) Cut-away view of a Swagelok check valve[17]

The final type of valve that is employed is a relief valve. A relief valve operates similar to a check valve, however it is used to ensure that the system will not over pressurize. Once a relief valve is set to a specific pressure, the valve will open if the pressure inside the line goes above that set value. **Figure 32** portrays a simple cut-away view of a standard relief valve that is provided by Swagelok.

[17] Image pulled from the Swagelok catalog (Swagelok, 2008b)

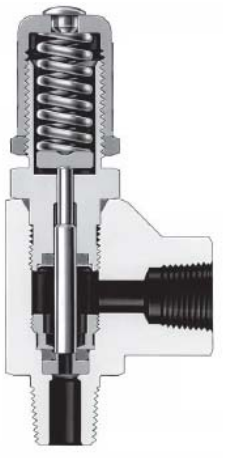

Figure 32) Cut-away view of a Swagelok relief valve[18]

4.2.2. FILTER

It is important in the design of the gas supply system to include a particulate filter to ensure that small solid particles of material from the irradiation chamber do not travel into other parts of the system. To achieve this, two particulate filters were used inline both upstream and downstream of the irradiation chamber. The filters are intended to remove particles that are greater than 0.5 microns. This will allow the fission gases to emanate through the filter while trapping small fragments, such as oxidization particles that may have somehow been released from the foil. The filter works by trapping incident particulates in a matrix material, therefore capturing large particles. The diagram by Swagelok (**Figure 33)** shows a cross sectional view of a typical inline filter with a sintered filer element.

[18] Image pulled from the Swagelok catalog (Swagelok, 2008c)

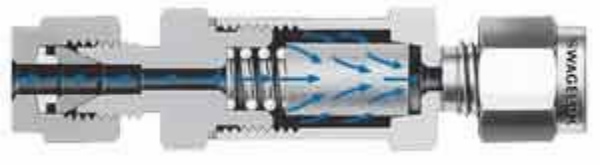

Figure 33) Cut-away view of a Swagelok inline filter[19]

4.2.3. MICROTUBING

Microtubing was used to connect the aluminum fission chamber to the gas supply system. The microtubing is constructed of stainless steel, with an outside diameter of 0.0625" ($\frac{1}{16}$") and an inside diameter of 0.03" with a length of 6". These dimensions resulted in a tube volume of 0.004 in^3 (0.066 cm^3). This small inside diameter will allow for the minimization of the active volume in the system. The role of minimizing the active volume is to restrict the dilution of the fission gas created during the collection process. The outside diameter of the microtubing drives the dimensioning of the air flow holes that are bored into the aluminum irradiation chamber. These holes must be smaller than the height of the open area inside the aluminum fission chamber where the actual HEU sample is placed to allow for a proper fit. One end of the microtubing is joined to the gas supply system through the use of the Swagelok tube fitting connection. The end of the tubing connected to the aluminum fission chamber is done so by using an

[19] Image pulled from Swagelok (Swagelok, 2008d)

epoxy resin hardener[20]. This epoxy, once heat cured, allows for a hermetic union between the aluminum and stainless steel.

4.2.4. VACUUM PUMP

A hand-held vacuum pump, similar to that pictured in **Figure 34,** was used to evacuate the active volume of both the apparatus and the detector volume to anticipate collection of the fission-gas sample. A hand-held pump is sufficient for this application since the total active volume is only approximately 7.0 cm^3 and that of the detector volume is 10.0 cm^3. With these relatively small volumes, evacuating the air from these spaces is easy with this device, and no large vacuum tool is necessary. This is also convenient since the vacuum pump may become contaminated with small traces of fission-product nuclides, such as cesium-137, and will need to be discarded after all the experiments have been completed. If a large device was in need of disposal because of contamination, higher costs would be incurred, thus the use of a small hand pump is cost effective.

[20] Armstrong Products Company A-12 Resin and Hardener

Figure 34) Hand vacuum pump[21]

4.2.5. DUMP TO FILTERED HOLD TANK

The system is designed so that when the vacuum pump is used to evacuate the volume of the apparatus, the purged air will be dumped into a filtered hood inside the reactor bay. Although it is anticipated that no activity will be released, any gas and/or particulates released are filtered through the fume hood and monitored.

4.2.6. NITROGEN CARRIER GAS

The irradiation apparatus has been designed such that during irradiation ambient air has been removed from the system and it remains at a vacuum. Once the irradiation has been completed however, the chamber will be purged with a nitrogen carrier gas to flush the fission gases downstream into the detector

[21] Image taken Gel-Pak (Gel-Pak, 2008)

collection device. Nitrogen was chosen because it is inexpensive, readily available, and has inert properties, so that it will simply push the fission gases downstream. Nitrogen is also primarily composed of nitrogen-14, which when activated creates nitrogen-15 which is also stable. This ensures that if any nitrogen is accidentally left inside the apparatus during subsequent neutron bombardment, it will not create a hazard from a health physics standpoint, nor will it affect the detector with an unwanted source.

4.2.7. PARTS LIST

The majority of parts used in the irradiation apparatus were obtained from the same supplier, Swagelok, to ensure uniformity. Other than Swagelok, some additional miscellaneous parts such as tubing and bolts were ordered from McMaster-Carr, however these parts could have been ordered from a wide range of distributors. **Table 6** is a complete list of the parts necessary to construct the fission apparatus. The list includes the part order number, the fitting size, as well as the body material type.

Table 6) Fission apparatus parts list

McMaster-Carr		
Description	**Tube Size**	**Part Number**
O-ring	2" x 1/16"	90025k427-33
Al Nuts	1/4"	90670A029
Al cap screws	1/4" x 1.5"	93306A546
Capillary Tube	1/16"	51755K35
Capillary Tube	1/8"	89785K113
Capillary Tube	1/4"	89895K121

Swagelok		
Description	**Tube Size**	**Part Number**
T union	1/4"	B-400-3
Ball Valve	1/8"	SS-41gs2
Ball Valve	1/4"	B-42s4
Check Valve	1/4"	B-4C-1
Filter	1/8"	SS-2F-05
Cross Union	1/8"	SS-200-4
Reducer	1/8" - 1/4"	SS-600-R-2
Reducer	1/4" - 3/8"	SS-600-R-4
Reducer	1/16" - 1/8"	SS-100-R-2
Pressure Gage	1/4" tube	PGI-63B-PC160-LAQX
Relief Valve	1/4"	SS-RL3S4

4.3. APPARATUS SUPPORT STRUCTURE

After assembling all of the components of the irradiation apparatus, the system was placed on a rigid support structure to allow for easy maneuverability, as well as consistency during irradiation. Since the support structure would not be irradiated directly, its composition, from an activation point of view, was not of concern. Thus, a thin sheet of stainless steel was used to create a platform for the apparatus, including the irradiation chamber. The image in **Figure 35** depicts the final assembled apparatus mounted to the stainless steel support structure.

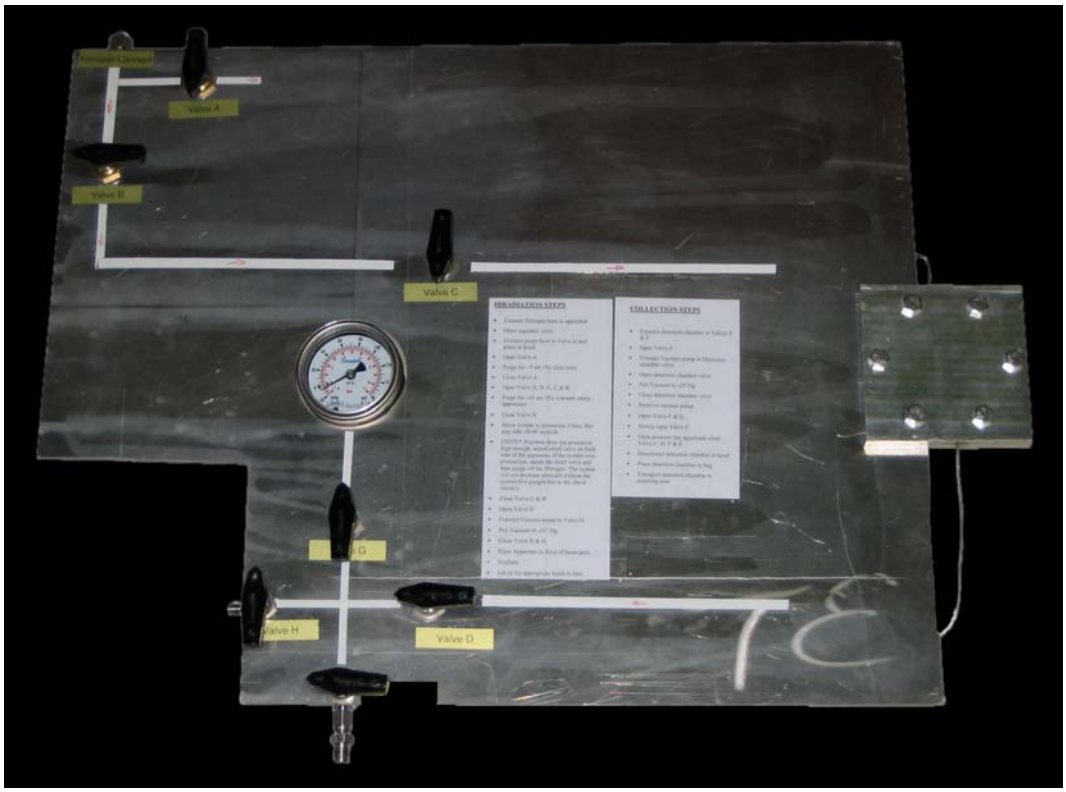

Figure 35) Apparatus with aluminum support structure

4.4. EXPERIMENTAL PROCEDURE

The following is a detailed procedure for conducting radioxenon collection using the HEU fission chamber in the Neutron Radiography Facility at Oregon State University. The procedure is allowed to vary if deemed necessary by the appropriate Reactor and Health Physics personnel for safety or operation reasons. The full step-by-step procedure can be located in **Appendix A**, however a summarized version will be included here for an understanding of the process necessary for fission product gas creation and capture. **Figure 36** depicts the

fission apparatus with the appropriate valve labels used for the experiment procedure.

Prior to the first irradiation, a vacuum test must be conducted to assure that the apparatus is hermetically sealed. For this test, the valve upstream of the fission chamber, **Valve C,** must be closed, as well as the valve downstream, **Valves F.** The closure of these valves assures that the vacuum area will include the fission chamber, as well as the connecting area to the detection chamber.

For the irradiation process, EXCEL must first be used to calculate the correct exposure time for the particular sample size desired. Next, the fission apparatus must be purged with nitrogen. To accomplish this, **all Valves,** excluding **Valve A**, must be open and the nitrogen gas must be turned on. This will allow the flow of nitrogen to remove any fission gases prior to the irradiation.

The nitrogen gas is then turned off, and the vacuum pump is used to remove all of the gas from the fission chamber. The removed gases are routed into a hold-up tank to confine the gases from the apparatus until they can be monitored prior to release. This will ensure that no hazardous fission products are released to the atmosphere.

After all of the nitrogen has been purged from the system, the fission apparatus is placed into the neutron beam and irradiated for the predetermined duration. Then, the fission chamber will rest to allow for the fission products to accumulate to the maximum cumulative yield. For xenon-133 this rest period is approximately sixty-seven hours, and has been calculated using STELLA. Then,

the detector is connected at the junction at **Valve E.** Once connected, **Valve E, F, G,** and **H** are opened. The vacuum pump is then initiated to purge the detector. **Valves H** and **G** are closed and the nitrogen is turned on. **Valves B, C** and D are opened in that order long enough for the detector to equalize pressure. At this point, the fission gas has been transported into the detector. The detection chamber is then isolated by closing **Valves E** and **F,** and disconnected. The detection chamber is then transported to the appropriate counting laboratory.

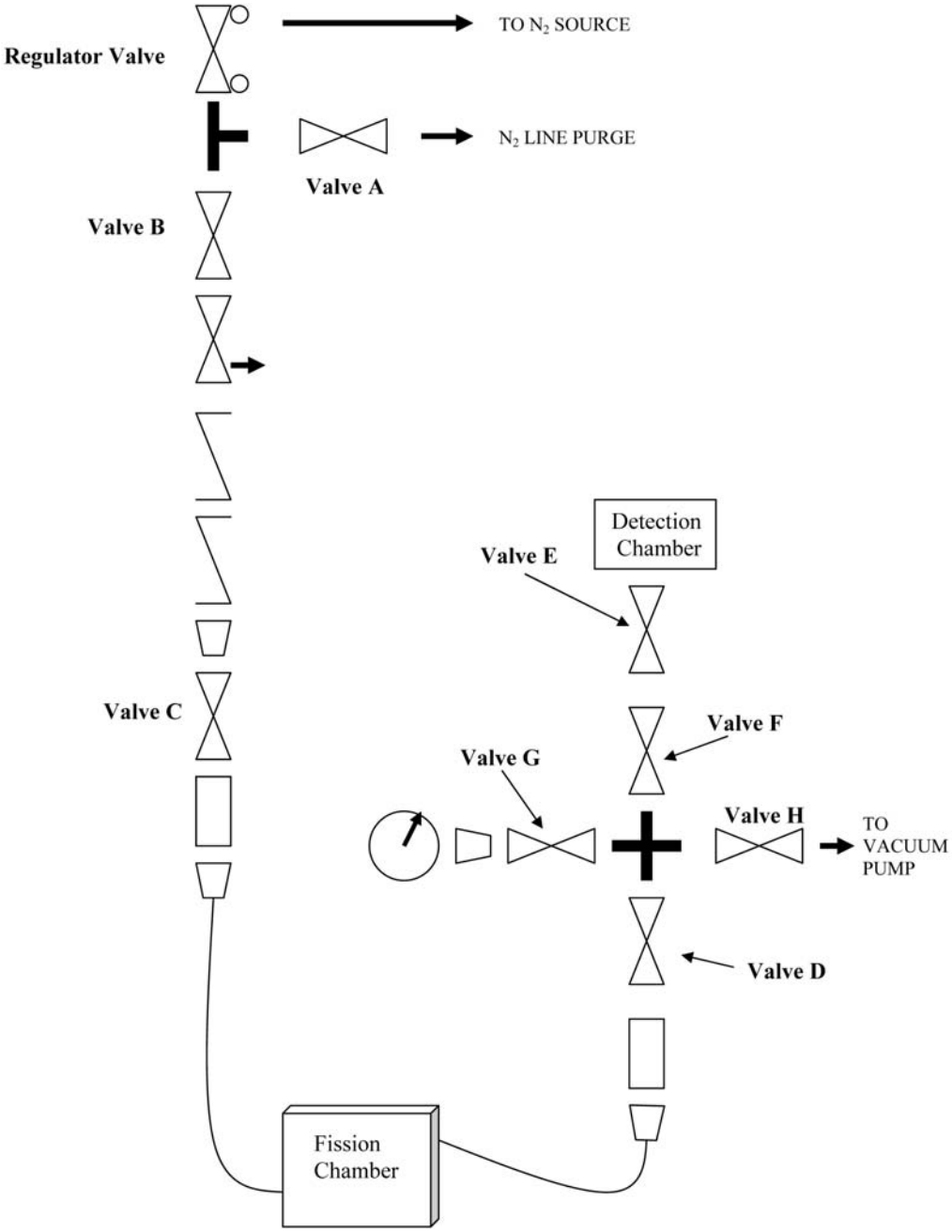

Figure 36) Valve diagram for the fission apparatus

5. MATERIALS AND METHODS

All of the calculations, as well as the method of isotope generation for this work, are described in detail herein. The topics in this section are presented in no particular order. Although some of the calculations presented are not highly pertinent to the actual generation of the radioxenon gas, they have been conducted to aid in the approval process of generating fission product gases in a research reactor.

5.1. FISSION RATE CALCULATION

The fission rate, FR, describes how many fission events are occurring in the HEU foil per unit time, and is the product of the flux, cross section, and number of atoms of uranium-235 present in the sample.

$$FR = \phi \cdot N \cdot \sigma$$

where N is equal to the product of Avogadro's number and sample mass, divided by uranium-235, the atomic number of uranium. Values for the parameters in the equation are as follows:

- Flux: $\phi = 4.74\text{x}10^{5}$ [n / (cm^2-s)] [22]
- Mass of 93% U-235: m = 0.20 [g] [23]

[22] This value of flux is pulled from the flux verification section of this work, and is used for all calculations.

[23] The mass of 0.20 grams is an estimated mass of the sample that was actually used. This approximation is used only to aid in the calculation process, and that other experiments may use different sample sizes.

- Thermal neutron cross section: $\sigma = 5.85 \times 10^{-22}$ [cm²]
- Atomic mass of U-235: A = 235[mol / g]
- Avogadro's number: 6.022x10²³ [atoms/ mol]

This yields the following result:

$$FR = 4.74x10^{5}\left[\frac{n}{cm^{2}-\sec}\right]\cdot 5.85x10^{-22}\left[cm^{2}\right]\cdot\frac{6.022x10^{23}\left[\frac{a}{mol}\right]\cdot 0.20[g]}{235\left[\frac{mol}{g}\right]}$$

$$FR = 1.42x10^{5}\left[\frac{fissions}{\sec}\right]$$

5.2. TOTAL FISSION-PRODUCT ACTIVITY CALCULATION

The calculation of the total fission-product activity was completed to characterize the overall decay rate of the irradiated HEU sample. It is interesting to note that the total activity is actually quantitatively related to the power of that material. Using this, the activity of the sample was calculated by first calculating the total power related to the HEU sample. The calculation of power is simply a conversion of the fission rate, knowing the average amount of energy that is released per fission.

$$Power\left[MW_t\right] = FR\left[\frac{fissions}{\sec}\right] x\left[\frac{200\,MeV}{1\,fission}\right] x\left[\frac{1.6\,x\,10^{-13}\,J}{1\,MeV}\right] x\left[\frac{1\,MW_t}{10^6\,J/\sec}\right]$$

The last two terms in the equation are merely unit conversions from MeV to joules and the conversion of watts to joules per second.

This yields a power for irradiation of the HEU sample of:

$$Power = 4.55\,x\,10^{-12}\left[MW_t\right]$$

The calculation of power is then used to find the total activity in the sample as follows:

$$Activity = 8.45\,x\,10^5\left[\frac{Ci}{MW_t}\right] x\,Power\left[MW_t\right] x\,Yield\left[\%\right] x\left(1 - e^{-\lambda_i t}\right)$$

where Yield is 100% for sum of all fission products and $e^{-\lambda_i t}$ is approximated as 0 to assume full saturation.

With this, the activity equation reduces to a function of the power:

$$Activity = 8.45\,x\,10^5\left[\frac{Ci}{MW_t}\right] x\,4.55\text{x}10^{-12}\left[MW_t\right]$$

$$Activity = 3.84\,\mu Ci$$

5.3. ***XENON ACTIVITY CALCULATION***

The calculation of the activity of xenon is dependent on the isotope of interest. Therefore, the only variable that depends on the chosen xenon isotope is the fission yield, and the isotopic half-life. The other parameter is the irradiation time, which can vary for every experimental procedure. The following are the standard parameter values for the calculation of specific xenon activities:

- Flux: ϕ = 4.74x10^5 [n / (cm^2-s)]
- Mass of 93% U-235: m = 0.20 [g]
- Thermal neutron cross section for fission of uranium-235: σ = 5.85 x 10^{-22} [cm^2]
- Atomic mass of U-235: A = 235 [mol / g]
- Avogadro's number: 6.022x10^{23} [atoms/ mol]
- Variable irradiation time: *t*[sec]
- Density of U-235: ρ = 19 [g / cm^3]
- Half-life of xenon isotope of interest: $t_{½}$ [sec]
- Cumulative yield of isotope at dependent time: %yield

Then, xenon activity is calculated using:

$$A_0[Bq] = \frac{m[grams] \cdot N\left[\frac{atoms}{cm^3}\right] \cdot \sigma[cm^2] \cdot \phi\left[\frac{n}{cm^2 - \sec}\right] \cdot t[\sec] \cdot \left[\frac{\%yield}{100}\right] \cdot \frac{\ln 2}{t_{1/2}[\sec]}}{\rho\left[\frac{grams}{cm^3}\right]}$$

$$\text{where: } N = \frac{Na \cdot m}{A}$$

It is relevant to note that the fission yield is dependent on the time allowed for decay post irradiation, but before the sample is collected from the irradiation chamber. After irradiation, the cumulative yield for specific nuclides increases to a maximum concentration. This concentration, or maximum build-up, is calculated using a decay model described in a subsequent section. Once the sample is collected from the irradiation chamber, build-in no longer occurs, so the activity of the sample will only decrease. The decrease in the sample activity will occur as described by the standard activity decay equation.

$$A(t)[Bq] = A_0[Bq] \cdot e^{-\lambda_x t}$$

$$\text{Where: } \lambda_x = \frac{\ln 2}{t_{1/2}}$$

- Initial activity: $A_0[Bq]$
- Decay time: t[sec]
- Isotope half-life: $t_{1/2}$ [sec]

Tabulated activities at the end of irradiation for a standard sample amount of 0.2 grams and various irradiation times have been calculated and are presented in **Table 7.** These values represent the maximum activity created during each irradiation for specific xenon isotopes. Attached in **Appendix E**, is a spreadsheet

formula to calculate the activity for all irradiation times between one minute and one hour.

Table 7) Tabulated activities of xenon isotopes based on irradiation time

Irradiation Time [sec]	Activity in mBq			
	Xe-131m	Xe-133	Xe-133m	Xe-135
5	0.50	278.48	14.89	2345.87
10	0.99	556.96	29.79	4691.71
15	1.42	835.43	44.68	7037.48
20	1.91	1113.91	59.57	9383.16
30	2.83	1670.87	89.36	14074.08
40	3.82	2220.68	118.76	18704.08
50	4.74	2777.63	148.54	23393.17
60	5.73	3327.43	177.95	28020.85

5.4. DOSE CALCULATION FROM ALUMINUM CHAMBER

When the aluminum chamber is irradiated, it becomes activated requiring that certain precautions are taken. When handling activated aluminum, if the proper decay time is not observed, the exposed individual may incur a significant dose. Therefore, a calculation of the aluminum activation is required to find the dose to an individual at a specific distance from the fission chamber.

To find the activity of the activated aluminum chamber, the mass must be calculated, but prior to this, the volume of the material must be determined. Once the mass is found, the total number of atoms of aluminum is calculated.

Volume:

$$V = l \text{ x } w \text{ x } h$$

$$V = 0.5\text{" x } 4\text{" x } 4\text{"} = 8\,\text{in}^3$$

$$V = 8\,\text{in}^3 \rightarrow 131.1\,\text{cm}^3$$

Mass:

$$m = V \text{ x } \rho$$

$$m = 131.1\left[cm^3\right] \text{x } 2.6989\left[\frac{g}{cm^3}\right] = 353.8[g]$$

Number of Atoms:

$$N_{Al} = \frac{m \text{ x } N_a}{M}$$

$$N_{Al} = \frac{353.8[\text{g}] \text{ x } 6.022\text{x}10^{23}\left[\frac{atoms}{mol}\right]}{26.982\left[\frac{g}{mol}\right]} = 7.897x10^{24}[atoms]$$

- Atomic Mass of Al-27: M = 26.982 [g / mol]

Now, knowing the exact number of aluminum atoms present during irradiation, the activity can be found. For the sake of this calculation, we will assume that the aluminum sample becomes saturated to assure a conservative estimation of the dose.

Activity:

$$A = \phi \text{ x } \sigma_{Al} \text{ x } N_{Al}\left(1 - e^{-\lambda t}\right)$$

- *Assume sample becomes saturated*

$$A = \phi \text{ x } \sigma_{Al} \text{ x } N_{Al}$$

$$A = 4.74\text{x}10^{5}\left[\frac{n}{cm^{2}\text{ - }s}\right]\text{x } 0.204\text{x}10^{-24}\left[cm^{2}\right]\text{x } 7.897\text{x}10^{24}\left[atoms\right] = 7.63x10^{5}\left[Bq\right]$$

- Flux: $\phi = 4.74\text{x}10^{5}$ [n / (cm²-s)]
- Averaged Al Cross section: $\sigma = 2.04 \text{ x } 10^{-23}$ [cm²]

$$A = 7.63x10^{5}\left[Bq\right] = 20.6[\mu Ci]$$

The next step is to calculate the photon flux emanating from the aluminum. Some general and conservative assumptions have to be made to determine this flux; the assumptions are listed below.

Flux from Al:

$$\phi_{Al} = \frac{S_A}{4}\ln\left(1 + \frac{R^2}{h^2}\right)\left(e^{-\lambda t}\right)$$

$$\text{where: } S_A = \frac{A}{4\pi} = 6.07x10^4\left[\frac{\gamma}{cm^2 - \sec}\right]$$

- Assume the 4" x 4" source is a disk source to obtain a radius, R, of 7.18 [cm]
- Assume h, the distance to the source, is 100 [cm]
- Assume t, the time after activation, is 10 [min]
- Half-life of Al: $t_{1/2} = 2.25$ [min]

With these assumptions, the flux calculation will be:

$$\phi_{Al} = \frac{6.07x10^4}{4}\left[\frac{\gamma}{cm^2 - \sec}\right] \cdot \ln\left(1 + \frac{(7.18[cm])^2}{(100[cm])^2}\right) \cdot \left(e^{-\frac{\ln(2)}{2.25[\min]}x10[\min]}\right) = 3.58\left[\frac{\gamma}{cm^2 - \sec}\right]$$

Now, with the flux, the dose rate imparted to an individual at 1 meter from gamma rays can be calculated.

Dose Rate:

$$\dot{D}_\gamma = \phi_{Al}\left[\frac{\gamma}{\mathrm{cm}^2 - \sec}\right] \cdot \left(\frac{\mu_{en}}{\rho}\right)_{tissue}\left[\frac{cm^2}{g}\right] \cdot E_\gamma[MeV] \cdot 1.6\mathrm{x}10^{-10}\left[\frac{J\text{-}g}{MeV\text{-}kg}\right]$$

Assuming a mass absorption coefficient of 0.0265 [cm^2 / g] in tissue and the photon energy is 1.779 [MeV].

$$\dot{D}_\gamma = \left(3.58\left[\frac{\gamma}{cm^2 - \sec}\right]\right)\cdot\left(0.0265\left[\frac{cm^2}{g}\right]\right)\cdot\left(1.779[MeV]\right)\cdot\left(1.6\text{x}10^{-10}\left[\frac{J\text{ - }g}{MeV\text{ - }kg}\right]\right)$$

$$\dot{D}_\gamma = 2.70x10^{-11}\left[\frac{Gy}{s}\right]$$

$$\dot{D}_\gamma = 2.70x10^{-11}\left[\frac{Gy}{s}\right]\text{x}\,10^{5}\left[\frac{mrem}{Gy}\right] = 2.70x10^{-6}\left[\frac{mrem}{s}\right]$$

$\dot{D}_\gamma = 0.00972\left[\frac{mrem}{hr}\right]$ at 1 meter, 10 minutes after irradiation.

Thus, the dose rate of 0.00972 mrem / hr will occur at 1 meter from the source, 10 minutes after irradiation has occurred. This dose rate is so minimal that for most radiological concerns it can be neglected. Also, the dose rate will continue to drastically decline over a relatively brief time due to the short half-life of aluminum-28. Note that the dose rate calculated does not account for photons that will be emitted as a result of being created as fission products. If these photons are of low energy, they may be appropriately shielded by the aluminum.

5.5. ATTENUATION CALCULATION

The calculation of attenuation is vital to account for the reduction in neutron flux on the HEU sample. Since the HEU sample rests inside an aluminum chamber, the neutron beam will be attenuated by a calculable fraction.

The total macroscopic cross section for aluminum-27 is tabulated to be 0.099 [cm^{-1}][24]. Therefore, the flux prior to attenuation through a thickness of 0.25 inches of aluminum (0.635 cm) is calculated as:

$$I = I_o e^{-\Sigma x}$$

$$\frac{I}{I_o} = e^{-(0.099 cm^{-1})(0.635 cm)}$$

$$\frac{I}{I_o} = 0.94$$

This reveals that the first half of the aluminum chamber attenuates the original neutron beam by approximately 6% before it strikes the HEU. Thus, it is vital to assure that the aluminum chamber is sufficiently thin so as to not overly attenuate the incident thermal neutron beam.

[24] From *Reactor Physics Constants,* ANL-5800 (Duderstadt, 1976c).

5.6. STELLA MODEL

STELLA is a compartmental model, developed by Isee Systems, used to model diverse dynamic systems. It was used in this project to determine the cumulative time-dependent yields, and maximum yields, for specific nuclides of fission. Determining the yields is vital in the calculation of the xenon activity produced.

The STELLA program is based on two main concepts; bins and converters. In the bin, an amount can be held, similar to a holding tank. If nothing is being added-to or removed-from the bin, the value will remain constant. However, if attached to the bin is a converter, the value in the bin can vary depending on the inputs and the equations governing the converter. For the model that has been created, the converters simply model the transformation, or decay, of one nuclide into another, as well as the creation of a nuclide from the fission process. **Figure 37** depicts the converters and bins used in the STELLA model of the 133 fission chain for example. The comprehensive STELLA model created can be viewed in **Appendix E**.

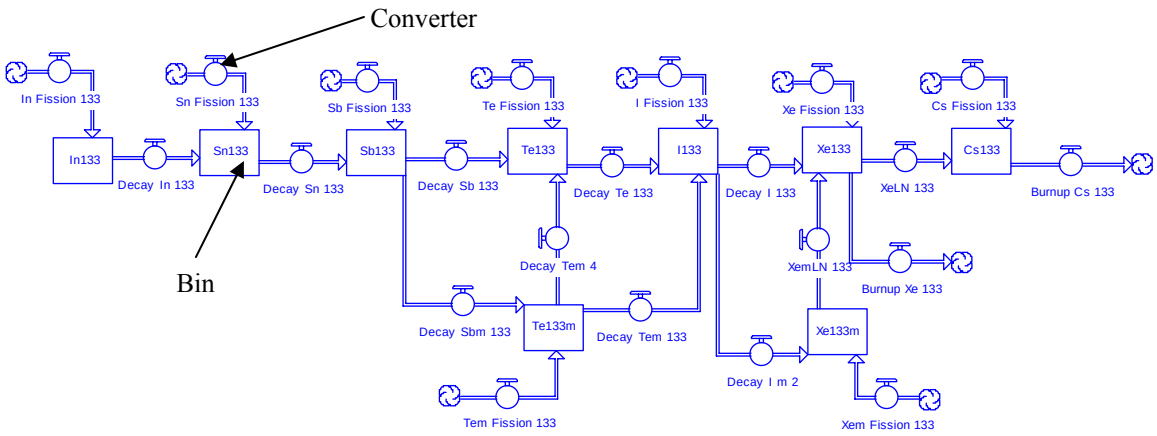

Figure 37) STELLA model of the 133 fission chain

The input information given to the STELLA model is straightforward. Since STELLA is a compartmental model, it was used here to simulate the series of decays that occurs after fission. The decay chains of interest for this model were the 83-89, 127, 129 and 131-138 decay chains. Of particular interest are the 131, 133 and 135 decay chains because they encompass the xenon isotopes of interest. The other decay chains were included to account for particular fission products of interest from a biological hazard standpoint, such as isotopes of iodine and cesium.

The specific information that was needed for model operation was the half-life of each nuclide and the independent fission yield[25]. Some nuclides decay through multiple branches, or into a metastable state. The flux was needed to allow for the burn-up of some of the longer-lived, highly absorbing nuclides. For this calculation, the neutron absorption cross section was also required.

[25] Information on fission product yields was obtained from Evaluation and Compilation of Fission Product Yields (England, 1993)

The STELLA model created to simulate the yield percentages has only one main user control input and that is the irradiation time from 0 to 1 hours. This was added to allow an unfamiliar individual to view the cumulative fission yields depending on irradiation time and sample collection time, because it has been anticipated that the gas samples may be collected at times other than at their peak yields.

5.7. FISSION MATERIAL SELECTION

Some consideration was taken when choosing the material that would be fissioned to create the xenon gas samples. After speaking with several individuals, it was decided that uranium-235 would be the best target material due to availability, knowledge of fission product production and ease of use. Other materials such as plutonium-239, uranium-238 or thorium-232 could have been used, however their fission yields are either less characterized, the material is of a greater proliferation risk and would be undesirable to obtain, or the material does not have a sufficient thermal neutron cross section.

5.7.1. ENRICHMENT JUSTIFICATION

It was decided that for ease of use, it would be best to use a highly enriched sample (>90% enrichment) for the fission target. This high enrichment of the material will allow for maximization of fission sites, while simultaneously

minimizing other intrusive material that will hinder the fission gas from escaping the material matrix. With a highly-enriched sample, there are less atom bonds blocking the fission gas from escaping through the material structure, because there is a reduction in the total number of atoms present. This will allow the maximum amount of gas to escape the foil and allow for a higher number of gas molecules to be collected. The high enrichment also reduces the active volume necessary to hold the HEU sample, which in turn reduces the overall size of the aluminum irradiation chamber.

5.7.2. COMPOSITION JUSTIFICATION (SOLID FOIL)

Uranium can exist in several compositions: a pure uranium solid; a solid oxide (uranium oxide - UO_2); a gas (uranium hexafluoride - UF_6); or a liquid (uranyl nitrate - $UO_2(NO_3)_2$). Although all of these forms are useful for the fissioning process, only the form of uranium in a solid is useful for the fission chamber designed. If a liquid or gas uranium solution was used, it would cause the sample to be dispersed with the fission gas causing not only a radiological concern, it would also remove the sample from the fission chamber. Since it is vital to reuse the sample several times, a solid must be used.

Since it is desired to collect the fission gas from the irradiated HEU, it is advantageous to use a very thin sample to allow for the maximum amount of surface area for the given sample mass. This will help to ensure that the fission

gases created are more readily able to escape the solid. **Figure 38** is an image of the uranium foil that is used for the irradiation experiments; a black oxide coating can be seen on the surface of the uranium metal.

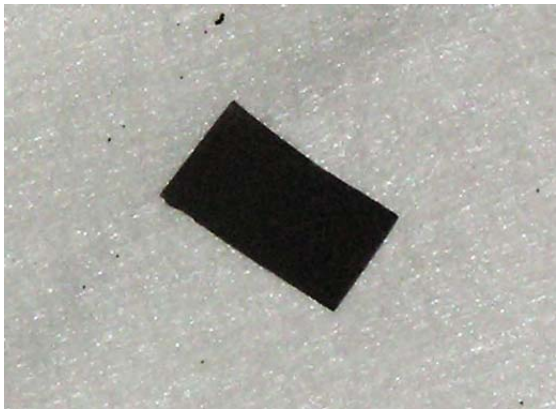

Figure 38) HEU foil sample with an oxidized surface

6. RESULTS

This section covers the findings of the experiments supporting this work. Information is presented in the chronological order in which it was collected. From the conducted experiments, it has been determined that the fission apparatus functions acceptably, incurring only one small hindrance during testing.

6.1. VACUUM TEST

After the system was manufactured and assembled, the system was purged to ensure that it could achieve a vacuum. It took only a few pumps from the hand-operated vacuum pump to achieve almost a complete vacuum, -25” Hg, on the system. Once the vacuum was achieved, it was closely monitored for two hours to ensure that it remained sealed.

Since the test was a success, the chamber was left at a vacuum while it was not in use. Approximately one month later, prior to the chamber being used to conduct the activation experiment, it was observed that the chamber was still at the vacuumed pressure. This confirms that the chamber will effectively be able to be in a state of vacuum while not in service to assure that no fission products may accidentally be released.

6.2. THERMAL NEUTRON FLUX DETERMINATION

It is important to characterize the flux that is incident on the HEU material so that precise estimates of fission gas can be obtained. To achieve this, a gold foil was irradiated inside the fission chamber designed to hold the HEU sample. After irradiation, the gold foil sample was counted using a 30% *high purity Germanium* (HPGe) spectrometer[26]. Two samples were irradiated during this verification, one bare gold foil, and one cadmium-encased gold foil. Two different samples were irradiated because the cadmium covering on the second sample will absorb the majority of the themalized neutrons that are bombarding the gold, thus only epithermal neutrons will be able to activate the gold. The difference in activity can then be taken from the bare gold foil sample and covered gold foil sample to back calculate the thermal and epithermal neutron fluxes.

The images in **Figure 39** and **Figure 40** show the detector used, as well as the interior of the detector cave where the sample counting occurs. In **Figure 40,** the calibration source for the detector can be observed. A europium-152 source with initial activity of 1.133μCi on February 1st of 1995 was used because of its 411.12 keV gamma ray. This nuclide was used to calibrate the detector since it has a photon energy similar to that of gold.

[26] **Appendix B** has the documentation related to this HPGe detector's efficiency.

Figure 39) View of HPGe detector

Figure 40) HPGe detector face

Prior to calibrating the detector, a background count of ten thousand seconds was conducted to characterize the background contribution to the source. Due to the highly shielded enclosure for the detector, little background activity was detected. The highest number of counts in any given channel was only around fifty counts.

A calibration source was then be used to calibrate the detector. The detection system interface uses software called Maestro – MCA Emulation Software to appropriately align the known energy from the calibration source to the detectors channels. **Figure 41** shows the results for the counting of the calibration source. The 411.12 keV peak from the europium-152 source occurs at channel 1983 and is highlighted in green in the figure. This data shows that the peak from the decaying activated gold foil will occur in the similar channels.

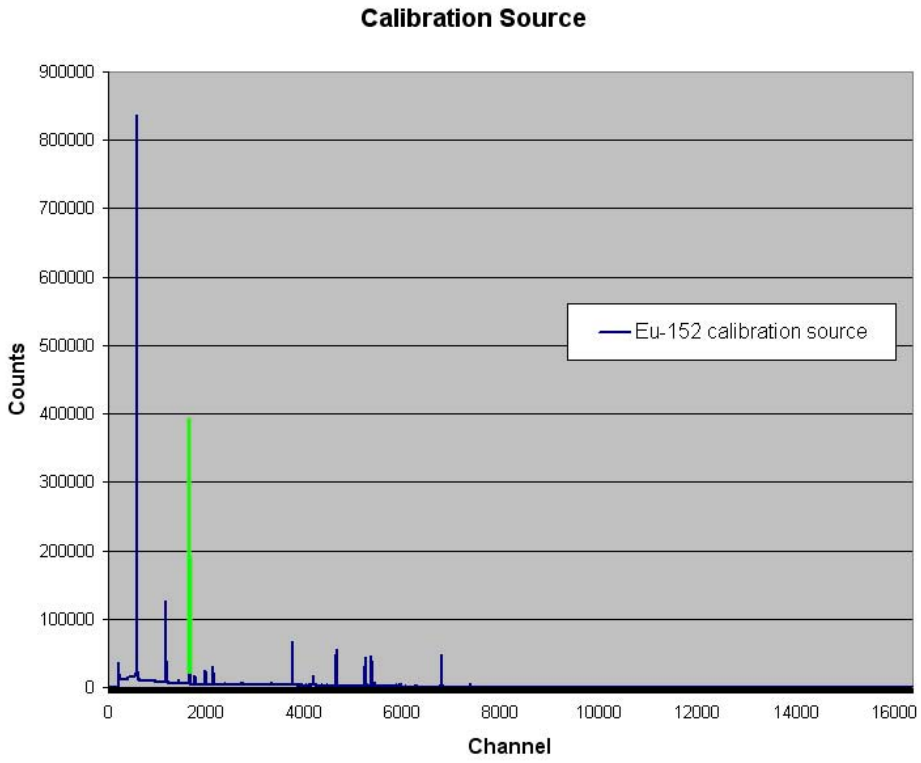

Figure 41) Calibration source results with 411.12 keV peak for 10,000 sec count

The data from the background counts can be used to subtract from the counts recorded from the gold foil, however due to the low background, this process was not necessary. The results from the ten thousand second live counts of the activated gold foils are displayed in the graph of **Figure 42** and **Figure 43,** for the bare and covered gold foil samples, respectively.

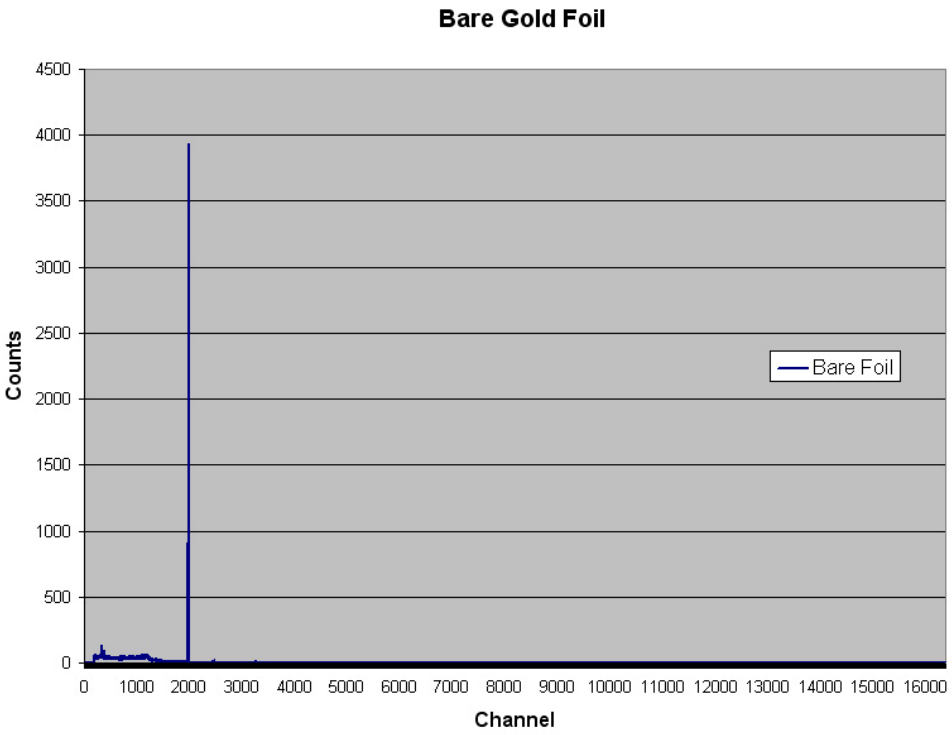

Figure 42) Bare gold foil counts for 10,000 sec count time

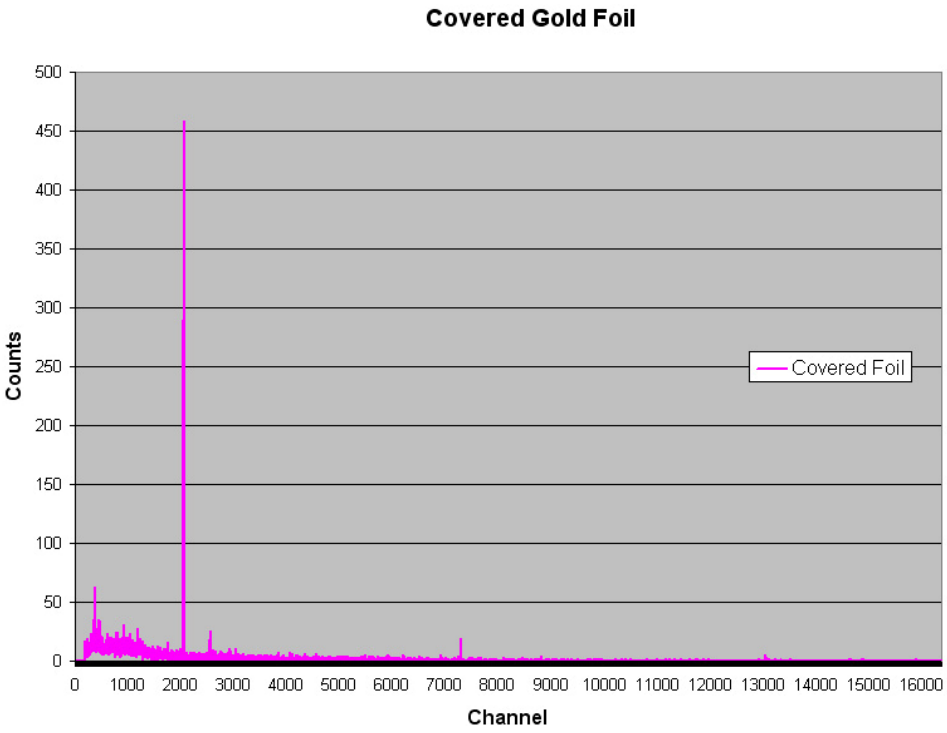

Figure 43) Covered gold foil counts for 10,000 sec count time

The results for the counts for the two samples are located in **Table 8.** The net count data can be used to calculate the neutron thermal and epithermal flux of the beam incident on the aluminum irradiation chamber.

Table 8) Gold foil activation count results for 10,000 sec counts

Detector	Net Counts	Error Net Counts
#121	28422	177
#381	2519	57

The error for the net counts is provided by the Maestro counting software and is calculated as:

$$\text{net area counting error} = \sqrt{(\text{gross area error})^2 + (\text{background error})^2}$$

6.3. FLUX CALCULATION

When the gold foil sample (gold-179) is bombarded with neutrons, it activates, absorbing a neutron creating gold-180, and then decaying by beta emission to mercury-180. **Figure 44** depicts the decay mechanism. When gold-180 decays by beta emission, it releases a characteristic gamma ray at 411.8 keV. The activity at the end of bombardment of the sample is calculated and the flux estimated. The *end of bombardment* (EOB) activity is the activity of the sample directly after the sample is finished being irradiated.

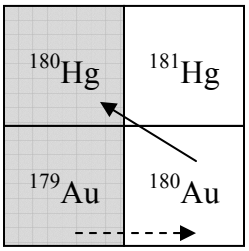

Figure 44) Gold activation decay mechanism

The EOB activity can be calculated using the following formula:

$$\text{EOB} = \frac{\frac{\ln 2}{t_{1/2}} \cdot \text{net counts}}{E_{ff} \cdot Y_{ield} \cdot \left(e^{(-\lambda \cdot t_1)} - e^{(-\lambda \cdot t_2)}\right)}$$

To determine the EOB activity, several factors must be known, such as the half-life ($t_{½}$) of the activated product, the net counts collected from the detector, the detector *efficiency* (E_{ff}), the yield percent of the gamma being detected (Y_{ield}), the time between the EOB and when the counting began (t_1), and the time when the counting ended (t_2).

The error for the EOB was calculated using the following:

$$\mathrm{EOB}_{\mathrm{error}} = EOB\sqrt{\left(\frac{A\sqrt{total\ counts}}{total\ counts}\right)^2 + \left(\frac{A\sqrt{E_{ff}}}{E_{ff}}\right)^2}$$

$$\text{where: } \mathrm{A} = \frac{1}{(\text{Count time})\cdot(\mathrm{Y_{ield}})}$$

The determination of flux following the EOB activity estimate has two components, the thermal and the epithermal contributions. The epithermal flux must first be calculated, and the results from it must be used to calculate the thermal flux. The epithermal flux is calculated as follows:

$$\phi_{\mathrm{epi}} = \frac{\mathrm{EOB}}{\mathrm{N_{atoms}}\cdot \mathrm{RI}\cdot\left(1-\mathrm{e}^{-\lambda\cdot \mathrm{t_{irr}}}\right)}$$

Since the EOB activity has already been calculated, there are only four other unknown values:

- number of atoms (N_{atoms}) in the original sample;
- resonance integral (RI) value;
- half-life of the activated material ($t_{½}$); and
- total time that the sample was irradiated (t_{irr}).

With this, the value of the epithermal flux can be determined. The error for the epithermal flux is as follows:

$$\phi_{epi_{error}} = \frac{\sqrt{\text{net counts}} \cdot \frac{\ln 2}{t_{½}}}{N_{atoms} \cdot RI \cdot \left(1 - e^{-\lambda \cdot t_{irr}}\right) \cdot E_{ff} \cdot Y_{ield} \cdot \left(e^{(-\lambda \cdot t_1)} - e^{(-\lambda \cdot t_2)}\right)}$$

The thermal flux is calculated using the following:

$$\phi_{th} = \frac{\frac{EOB}{N_{atoms} \cdot \left(1 - e^{(-\lambda \cdot t_{irr})}\right)} - RI \cdot \phi_{Epi}}{\sqrt{\pi/2 \cdot \sigma_{th}}}$$

The only new value that must be obtained for this formula is the counterpart for the resonance integral, the thermal cross section (σ_{th}). The error for the thermal flux calculation can be found using:

$$\phi_{th_{error}} = \sqrt{A^2 net\ counts + B^2 \phi_{Epi}}$$

$$\text{where: } A = \frac{\ln 2}{t_{\frac{1}{2}} \cdot N_{atoms} \cdot \sqrt{\pi/2\,\sigma_{th}} \cdot \left(1 - e^{-\lambda \cdot t_{irr}}\right) \cdot E_{ff} \cdot Y_{ield} \cdot \left(e^{(-\lambda \cdot t_1)} - e^{(-\lambda \cdot t_2)}\right)}$$

$$\text{and } B = \frac{RI}{\sqrt{\pi/2\,\sigma_{th}}}$$

The error that is incurred is due to the detectors efficiency, or ability to count the incident radiation events, as well as errors in the determination of the activity. Error was not given to values such as cross sections, time, and other units that for the purpose of this work were considered to be constants.

The calculated values therefore of thermal and epithermal flux, and the error associated with them, are located in **Table 9.**

Table 9) Thermal and Epithermal flux results with associated error

	Flux [n / cm² - s]	Error [n / cm² - s]
Thermal	4.74×10^5	4.98×10^3
Epithermal	3.61×10^3	3.79×10^1

6.4. ARGON ACTIVATION

Activation of an argon sample was necessary to demonstrate that the XEPHWICH detector operates appropriately when responding to a radioactive gas. A small sample of argon-40 gas therefore was activated and injected into the

XEPHWICH detector for counting purposes. Although the activated argon gas has much higher decay energies than those of the xenon isotopes that will be generated by the fission chamber, the activated gas was used to show that the detector operates properly. **Figure 45** shows a resultant signal pulse from the argon gas decay energy deposited into the XEPHWICH detector. This simple action shows that the XEPHWICH detector can count a radioactive gas. It also shows that the aluminum end cap used for the detector counting volume reflects sufficient light as to not hinder the counting process.

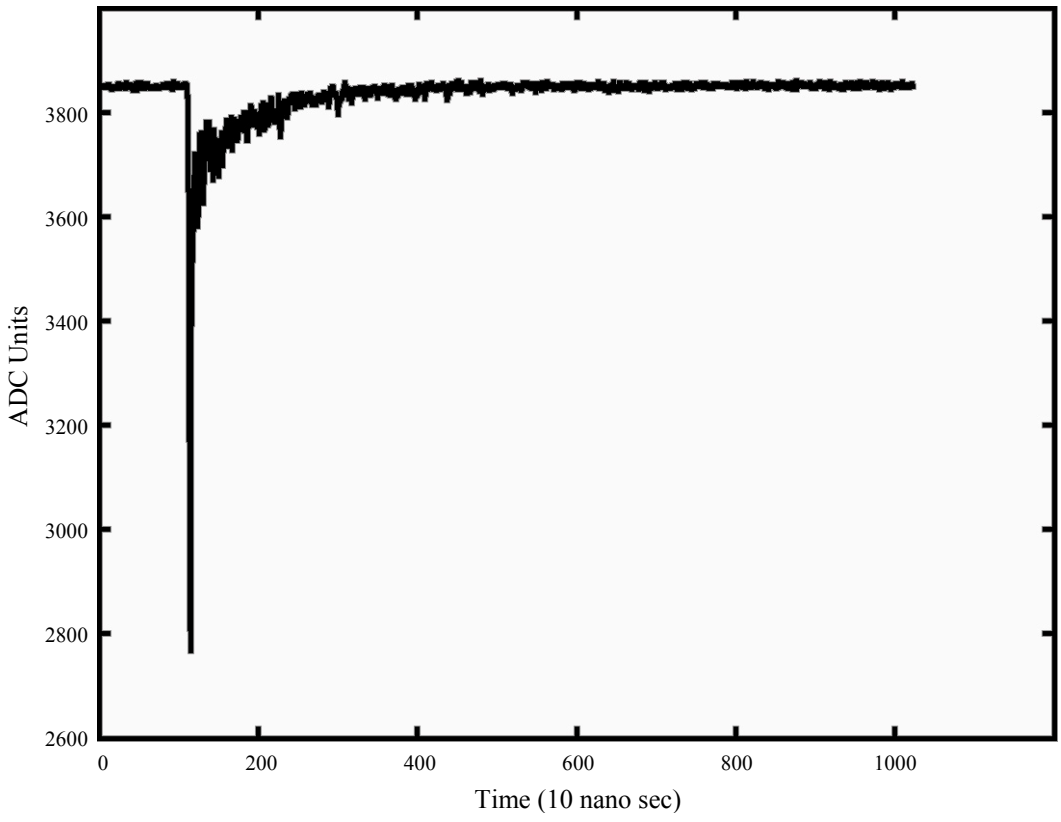

Figure 45) XEPHWICH detector pulse from argon-41 gas

A total of 10,000 raw signal pulses were captured during the test. These raw signals were then analyzed at a later date to create separate beta and gamma energy spectra. **Figure 46** and **Figure 47** shows the gamma and beta spectra for the decaying argon-41, respectively. These results are anticipated to be similar to the results for the xenon spectrum.

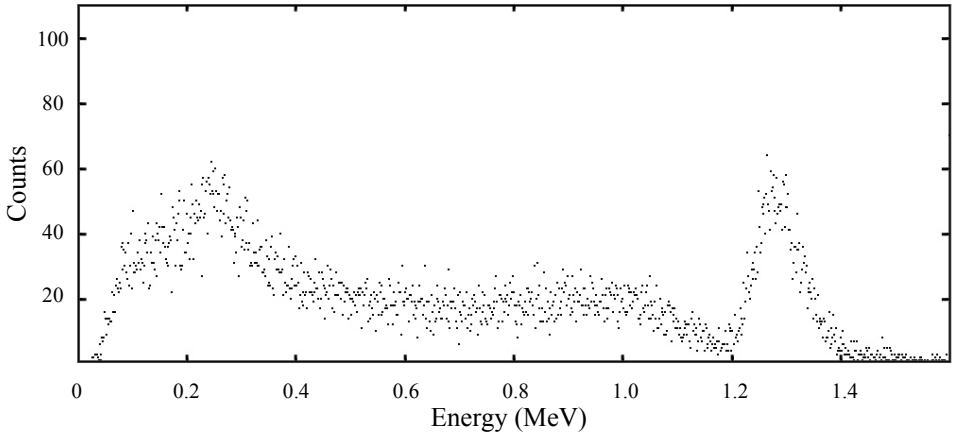

Figure 46) Gamma spectrum for argon-41 obtained with XEPHWICH

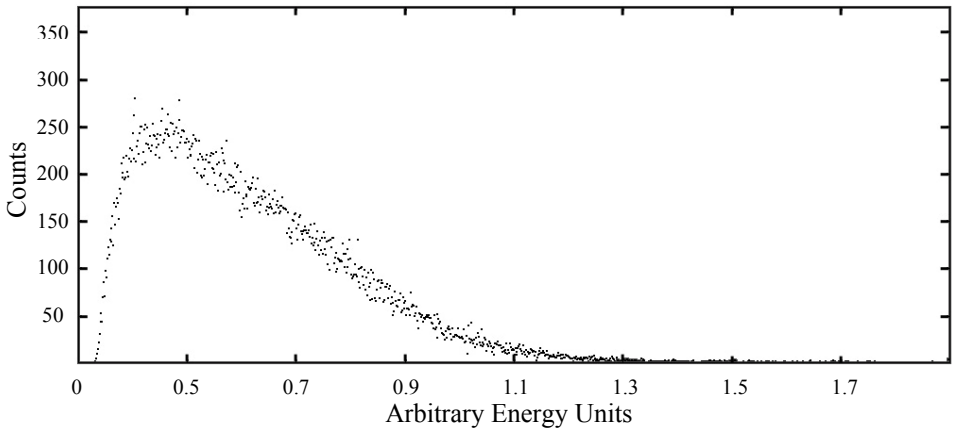

Figure 47) Beta spectrum for argon-41 obtained with XEPHWICH

6.5. XENON GENERATION

The first HEU irradiation to obtain xenon gas occurred on May 9th 2008. This was a 20 minute irradiation, with the expected production of approximately 900 mBq of xenon-133. Three days after end of bombardment, nitrogen gas was used to purge the system to collect the xenon isotopes. The gas was then counted using the newly created XEPHWICH detector.

6.5.1. COUNTING OF RESULTANT GAS

Using the XEPHWICH detector developed by Oregon State University, evidence of the production of radioxenon could be observed. Xenon-133 was the most prominent xenon isotope present due to the 66 hour build-in time allowed after irradiation. However, traces of xenon-135 could also be observed in the counting gas. These isotopes were identified by their characteristic decay energies. **Table 10** lists the four nuclides of interest with their decay modes and energies. They are all identifiable by the 30 keV x-ray followed by a gamma ray emission.

Table 10) Radioxenon prominent decay energies and modes

Isotope	x-ray energy [keV]	γ-ray energy [keV]
xenon-131m	29.62	163.93
xenon-133m	29.62	233.22
xenon-133	30.80	80.997
xenon-135	30.80	249.77

The XEPHWICH detector was used to collect 100,000 pulses over a time-span of about 7 hours. Although the activity of the sample was relatively low, the 80 keV gamma-rays from xenon-133 are easily distinguishable, as well as the 250 keV gamma from the xenon-135. **Figure 48** depicts the gamma-ray peaks that are incident in the sodium-iodide (NaI) layer of the detector. The 80 keV and 250 keV peaks are circled in red and blue, respectively.

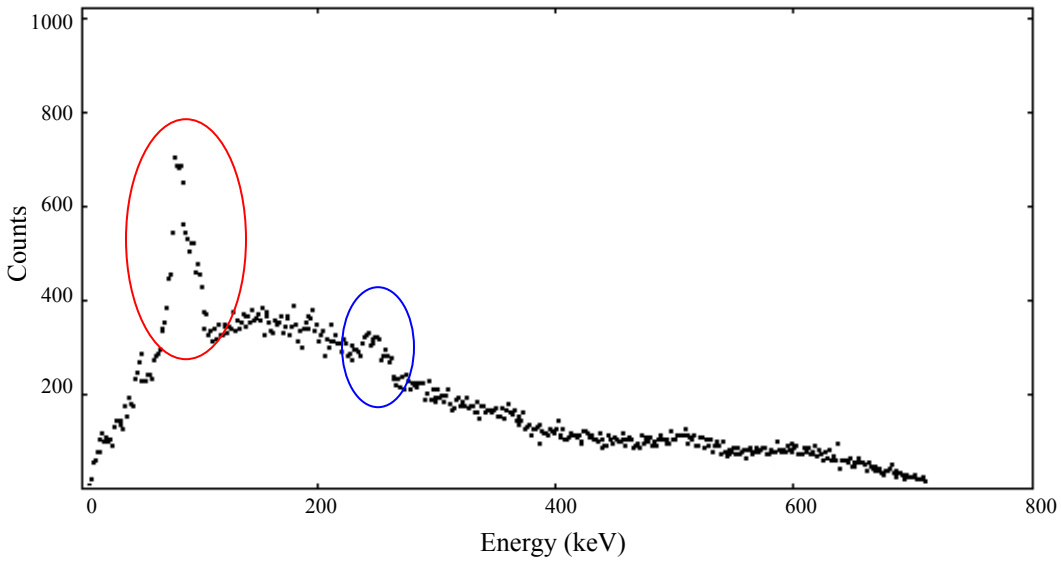

Figure 48) XEPHWICH radioxenon gamma spectrum results.

The beta and x-ray specific portions of the detector output were individually recorded for this test and are located below. The 30 keV x-ray is less distinguishable in this spectrum, but is presented to show the relative low activity. The results for the CaF_2 organic scintillator and the BC-400 plastic scintillator are located in **Figure 49** and **Figure 50,** respectively.

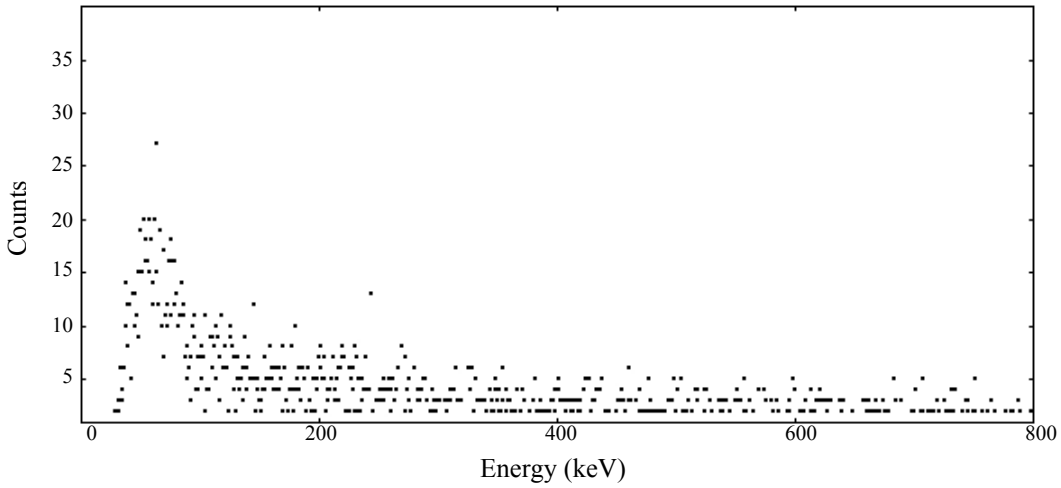

Figure 49) XEPHWICH radioxenon CaF_2 portion beta spectrum.

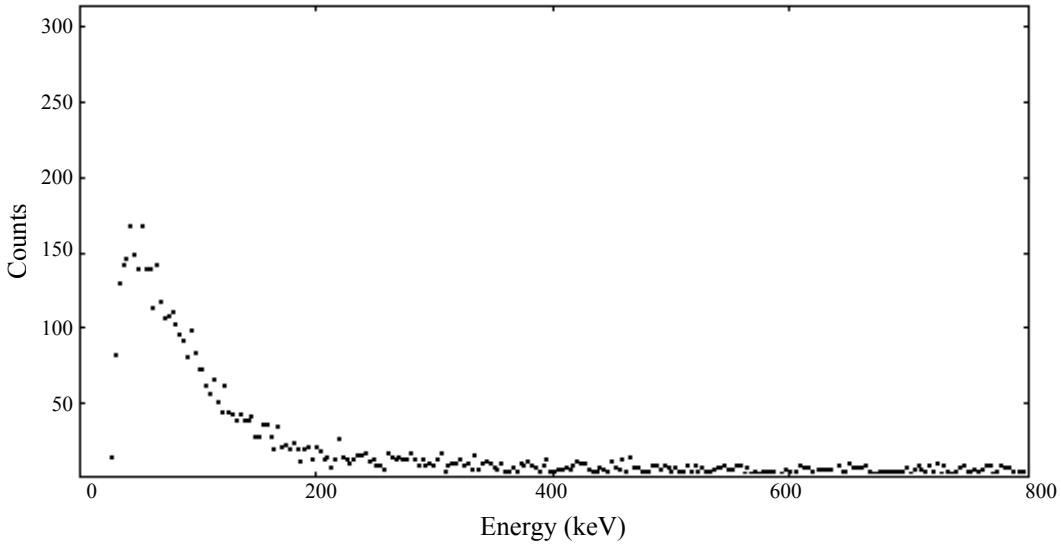

Figure 50) XEPHWICH radioxenon BC-400 portion beta spectrum.

7. DISCUSSION

7.1. OVERALL GENERATION SUCCESS

The observed results of the first irradiation experiment and subsequent counting using the XEPHWICH detector confirm that there was production of radioxenon isotopes, and that their transfer via nitrogen gas to the detection chamber was successful. Although the total activity transferred is questionable, xenon-133 and xenon-135 were confirmed to be present in the sample. The generation of greater activities can be obtained by lengthening the irradiation time in subsequent exposures.

7.2. GENERATING EFFICIENCY ERRORS

Our results indicate that the amount of radioxenon gas created and the amount of gas detected is inconsistent. This loss in the radioxenon is due to several underlying factors. First, a fraction of the activity remains in the gas in the active volume of the apparatus. Only about two-thirds of the nitrogen that purged the radioxenon from the foil was transported to the detector.

Secondly, only a portion of the gas escaped the HEU foil. The remainder of the gas remains trapped in the foil matrix. The ratio of loss from the active volume versus the gas trapped in the foil can be found by varying the active

volume of the transported gas, because the loss due to the gas trapped in the foil matrix will remain constant.

Another possible loss mechanism could be electroplating of the xenon onto the inside of the fission apparatus and the piping walls. If gas becomes electro-statically charged, it may adhere to the metals inside the chamber.

The detector efficiency also accounts for some of the discrepancy for the quantity of radioxenon activity detected. At this time the efficiency of the XEPHWICH detector has yet to be determined. The current goal for the detector is to observe coincidence radiation events emitted from the decay of the four xenon isotopes of interest. This therefore means that the overall system efficiency cannot be determined at this time. At a future date it will be possible to easily determine the overall efficiency of the radioxenon generation process, once the detector has been properly characterized.

A slight deviation for this experiment may also occur from the varying neutron flux. Although much effort was taken to align the apparatus with the neutron beam identically to the flux verification experiment, it is possible that the chamber may be slightly misaligned. A jig was used to alleviate this problem to attempt to make results as consistent as possible.

The activity of the radioxenon sample has yet to be determined since the detector is still in the optimization phase. It has been determined by the general rate of decay incidences however, that the activity is significantly lower than

initially predicted. This therefore means that some of the loss mechanisms could be further investigated to account for the removal of the radioxenon gas.

7.3. LIFETIME USE OF GAS

As previously mentioned, the xenon gas will be collected from the fission apparatus approximately 3 days post irradiation to allow for the proper accumulation of xenon-133. Based on the experimental procedure submitted to the *Reactor Operations Committee* (ROC*)* of the *Oregon State TRIGA Reactor* (OSTR), the gas will then be counted with the XEPHWICH detector and will remain inside the detector cap after counting until the appropriate decay time (60 days) has passed. The counting duration for each sample is unspecified, as the length of the collection process will be determined by the amount of events desired to be collected.

Currently, each HEU sample has been restricted to an arbitrary limit of five total irradiations. This limit was chosen with the understanding that each sample would be irradiated for 1 hour at each exposure. However, the actual irradiation durations are approximately one-third of this time. Since the irradiation time is less than previously considered, it may be possible to irradiate each sample approximately fifteen times.

It is possible that each sample may also be counted for more than one collection period. Since it will take a substantial time (~2.5 months) for all of the

xenon to decay, it is possible to conduct several trials during this time. However, due to the different decay times for each of the four xenon isotopes of interest, the concentrations of one xenon nuclide to another will vary as the sample ages.

It may also be possible to amend the OSTR experimental procedure to allow for longer duration irradiations if it is deemed necessary to create a higher activity sample. Since the potential tissue dose associated with the current irradiation time is so minimal (several orders of magnitude less than dose limits) a longer irradiation time would be inconsequential to radiological risk.

After the sample has been counted and is no longer needed, the gas will be released from the detector into the fume hood. This will only occur after the appropriate decay time has occurred. Residual traces of gas will also be present prior to irradiation in the fission apparatus, and must be removed prior to subsequent irradiation. For this, the system is purged with nitrogen, and the expelled gas is again released through the fume hood.

7.4. TOTAL IRRADIATIONS EXPECTED

It is anticipated that each foil will be irradiated the maximum permissible amount to reduce the amount of radioactive waste that needs to be disposed, as well as reduce the overall cost. Each new HEU foil sample will be placed in a new aluminum irradiation chamber, so the fabrication of additional flanges is necessary for ongoing experimentation. The fabrication of new irradiation

chambers is to ensure that the HEU material will not be handled once it has been irradiated. By discarding the HEU inside the irradiation chamber, the sample will be entombed inside this device. This can be achieved by simply capping the ends of the irradiation chambers microtubing that connects to the reducer sections. Since the sample will be not destroyed, it may be possible to retrieve the entire device if additional irradiations are deemed acceptable.

A detailed record of irradiation dates and durations has been created (see **Appendix F**) for each foil sample. After all irradiations have been completed, this data can be used to calculate the total activity created due to the fission process. This value of activity will be used to ensure the foil is within the proper limits for disposal.

7.5. OBTAINING APPROVALS

Several approvals were needed during the process of obtaining material and conducting an experiment using HEU and the Oregon State TRIGA Reactor. The process of obtaining these approvals was arduous to say the least, with some of them taking several months to obtain. One lesson to take away from this process is to attempt to minimize the restricting factors for any experiment. Specific to the generation of xenon, an arbitrary limit of 1 hour was used for an irradiation time limit. This limit currently restricts the generation of greater quantities of radioxenon gas if it is deemed necessary, and has no practical

justification since the activities created would be well below any significant amount of radiological concern.

The majority of the time of this project was spent waiting for appropriate approvals to both run the experiment and obtain the HEU material. Overall, the approval process took approximately six to nine months to obtain before the actual experiment could occur.

8. CONCLUSION

The work that has been completed for the generation of radioxenon gas has encompassed a wide range of aspects. It not only included administrative duties such as obtaining necessary approvals, but also calculation requirements to find necessary information regarding the activities of xenon to be created. This work also included hands on design and fabrication of an apparatus for the sole purpose of the generation of xenon. It has also been demonstrated that xenon gas can be generated using the apparatus designed and fabricated.

Many aspects of this work can be improved by simple variations to allow for a better overall final product. The fission apparatus itself would be better suited if the following considerations would be made.

1. Reduce the active volume of the apparatus by minimizing the irradiation chamber volume and eliminating redundant valves and excess tubing.
2. Use a more refined relief valve so the adjustment to the appropriate pressure is easier.
3. Replace ball Valve C with a needle valve so that during the purging process the transfer of gas can be achieved slower.
4. Obtain a low pressure regulator rather than a flow regulator for the nitrogen source to achieve better control of the gas flow.

5. Edit the procedure to account for changes that occurred during the actual experimental process.

It may be possible to find other areas of improvement, such as creative ways to expedite several of the approval processes; however the items listed are a practical solution to some of the troubles that occurred during the experimental process.

Although all of the goals for this project have been met, it may be possible to further experiment and understand and characterize complications in the generation of radioxenon gas that occurred over the duration of this work; specifically, accounting for the loss errors that are associated with obtaining a fission product gas from a metal HEU foil, as well as the transportation mechanism that was used.

BIBLIOGRAPHY

American Elements. Xenon. Available at: http://www.americanelements.com/xe.html. Accessed 4 April 2008

Cember, Herman. Introduction to Health Physics Third Edition. New York: McGraw-Hill; 294295; 1996a

Cember, Herman. Introduction to Health Physics Third Edition. New York: McGraw-Hill; 310-311; 1996b

Cember, Herman. Introduction to Health Physics Third Edition. New York: McGraw-Hill; 152-154; 1996c

Comprehensive Nuclear-Test-Ban-Treaty (CTBT). Available at: http://www.ctbto.org/. Accessed 10 February 2008

Covidien Imaging Solutions. Xenon Xe 133 Gas. Available at: http://www.imaging.mallinckrodt.com/Products/Product.asp?ProductID=53. Accessed 4 April 2008

Daily Med. Xenon Gas Description. Available at: http://dailymed.nlm.nih.gov/dailymed/drugInfo.cfm?id=6064. Accessed 4 April 2008

Duderstadt, J., Hamilton, L. Nuclear Reactor Analysis. John Wiley & Sons, Inc.; 18-19, 1976a

Duderstadt, J., Hamilton, L. Nuclear Reactor Analysis. John Wiley & Sons, Inc.; 57, 1976b

Duderstadt, J., Hamilton, L. Nuclear Reactor Analysis. John Wiley & Sons, Inc.; 606-609, 1976c

Elements Database. Periodic Table. Available at: http://www.elementsdatabase.com/. Accessed 11 March 2008

England, T.R., and B.F. Rider. Thermal Neutron Induced Fission. Los Alamos National Laboratory, LA-UR-94-3106; ENDF-349 (1993).

ENSDF. Evaluated Nuclear Structure Data File. Database version of 5 April 2007; www.nndc.bnl.gov/ensdf

Gel-Pak. Hand Pump. Available at: http://www.gelpak.com/images/handvacuumpump-sm.jpg. Accessed 9 March 2008

Knoll, Glenn. Radiation Detection and Measurement Third Edition. Chichester: John Wiley & Sons, Inc.; 219-220, 2000a

Knoll, Glenn. Radiation Detection and Measurement Third Edition. Chichester: John Wiley & Sons, Inc.; 58-59, 2000b

Knoll, Glenn. Radiation Detection and Measurement Third Edition. Chichester: John Wiley & Sons, Inc.; 553-554, 2000c

Knoll, Glenn. Radiation Detection and Measurement Third Edition. Chichester: John Wiley & Sons, Inc.; 9-10, 2000d

Lilley, John. Nuclear Physics Principles and Applications. Chichester: John Wiley & Sons, Inc.; 7-8, 2001a

Lilley, John. Nuclear Physics Principles and Applications. Chichester: John Wiley & Sons, Inc.; 155-116, 2001b

Lilley, John. Nuclear Physics Principles and Applications. Chichester: John Wiley & Sons, Inc.; 29, 2001c

Lilley, John. Nuclear Physics Principles and Applications. Chichester: John Wiley & Sons, Inc.; 144-147, 2001d

Lilley, John. Nuclear Physics Principles and Applications. Chichester: John Wiley & Sons, Inc.; 16-17, 2001e

Lilley, John. Nuclear Physics Principles and Applications. Chichester: John Wiley & Sons, Inc.; 264, 2001f

Los Alamos National Lab (LANL) Chemistry Division, Periodic Table of the Elements, Xenon. Available at: http://periodic.lanl.gov/elements/54.html. Accessed 22 February 2008

Marco Rubber. Buna-N (Nitrile) O-Rings. Available at: http://www.marcorubber.com/buna.htm. Accessed 15 May 2007

McIntyre, J. I., T. W. Bowyer, J. C. Hayes, T. R. Heimbigner, S. J. Morris, M. E. Panisko, K. W. Pitts, S. L. Pratt, P. L. Reeder and C. W. Thomas (2003). Generation of Radioxenon Isotopes, technical report PNNL-14338.

McMaster-Carr. Available at: http://www.mcmaster.com/catalog/114/gfx/small/6540kc1s.gif. Accessed 9 March 2008

Murray, Raymond. Nuclear Energy an Introduction to the Concepts, Systems, and Applications of Nuclear Processes Fifth Edition. Boston: Butterworth-Heinemann; 45-46; 2001

Shultis, K., Faw, R. Radiation Shielding. La Grange Park: American Nuclear Society, Inc.; 2000

Swagelok. Available at: http://www.swagelok.com/images/cmi/_Valves/AFS-cutaway.jpg. Accessed 9 March 2008a

Swagelok. Available at: http://www.swagelok.com/downloads/webcatalogs/EN/MS-01-176.PDF. Accessed 9 March 2008b

Swagelok. Available at: http://www.swagelok.com/downloads/webcatalogs/EN/MS-01-141.pdf. Accessed 9 March 2008c

Swagelok. Available at: http://www.swagelok.com/images/cmi/_Filters/Fcut.jpg. Accessed 9 March 2008d

United States Nuclear Regulatory Commission (U.S. NRC). Fission Gases. Available at: http://www.nrc.gov/reading-rm/basic-ref/glossary/fission-gases.html. Accessed 9 February 2008

APPENDICES

APPENDIX A – EXPERIMENTAL PROCEDURE

The following is a detailed procedure to be followed when conducting radioxenon collection using the HEU fission chamber in the Neutron Radiography Facility. With prior Reactor Supervisor and Senior Health Physicist approval, these steps may be modified to achieve the safest and most efficient gas-collection procedure. Changes to the procedure shall be captured by experiment revisions.

Pre-irradiation Procedure

1. Equalize chamber to atmospheric pressure by bleeding the nitrogen purge valve.
2. Remove the six bolts on the aluminum irradiation chamber.
3. Insert HEU using proper handling techniques.
4. Tighten the six aluminum bolts on the irradiation chamber.
5. Install the fission chamber in the test apparatus.
6. Verify all apparatus valves are shut.
7. Verify that vacuum pump discharge is directed to a hold-up tank. Whenever a uranium sample is installed in the test apparatus, the vacuum pump discharge must be directed to a hold-up tank when the pump is running.
8. Conduct a vacuum drop test to verify the integrity of the sample holder and attached apparatus as follows
    a. Open Valves B, C, D, F, G, H.
    b. Turn on the vacuum pump and run the pump until system vacuum is at least 25” Hg.
    c. Shut Valve H and turn of the vacuum pump.
    d. Observe system vacuum and verify system vacuum does not decrease by more than 1.0” Hg vacuum over five minutes. For example, if initial vacuum in 26” Hg and does not drop below 25” Hg in five minutes then the vacuum test is successful.

Irradiation Procedure

1. Using the STELLA model in conjunction with EXCEL formulations, calculate the appropriate irradiation time and decay time for desired sample.
    a. Open the xenon gas EXCEL sheet.
        i. Locate the proper irradiation time that corresponds to the desired activity of the xenon isotope of interest.
        ii. Record the irradiation time.
        iii. Record the decay time.
    b. Open the xenon gas model in STELLA.
        i. Insert the irradiation time located from the EXCEL sheet.

   ii. Observe when the maximum yield occurs for the fission isotope of interest.
   iii. Verify that the calculation for the STELLA decay time, and the EXCEL decay time correspond.
2. Check that all of the fittings are secure on the fission chamber, and that all valves are closed.
3. Verify vacuum pump discharge is directed to the hold-up tank.
4. Verify hold-up tank pressure is at least ten pounds below rated tank pressure. If tank pressure is not at least ten pounds below rated tank pressure, then the tank should be vented to a hood per SHP direction or a different tank should be installed.
5. Connect nitrogen supply
6. Open nitrogen **regulator valve**
7. Open **Valve A.**
8. Purge for 10 seconds
9. Close **Valve A**.
10. Open **Valve H, D, G, C & B** in sequential order
11. Purge nitrogen gas for 1 minute.
12. Close **Valve H.**
13. Allow system to pressurize to 5 bar.[27]
14. Close **Valve C & B**
15. Open **Valve H**
16. Connect vacuum pump to **Valve H**
17. Pull Vacuum to -26" Hg
18. Close **Valve D & H**
19. Place apparatus in line of beam port
20. Irradiate for predetermined time
21. Let apparatus sit for predetermined build-in time
22. Connect detection chamber to **Valve E & F**
23. Open **Valve E**
24. Connect vacuum pump to detection chamber valve
25. Open detection chamber valve
26. Pull vacuum to -25" Hg
27. Close detection chamber valve
28. Remove vacuum pump
29. Open **Valve F & D**
30. Slowly open **Valve C**
31. Let pressure equalize
32. Close **Valve C, D, F & E**
33. Disconnect detection chamber under fume hood

[27] Note, if system does not pressurize high enough, adjust the relief valve on the back side of the apparatus. If the system over pressurizes, adjust the relief valve and then purge off the nitrogen. The system will not decrease pressure without the system first purged due to the check valves.

34. Place detection chamber in plastic bag for transport
35. Take to counting area

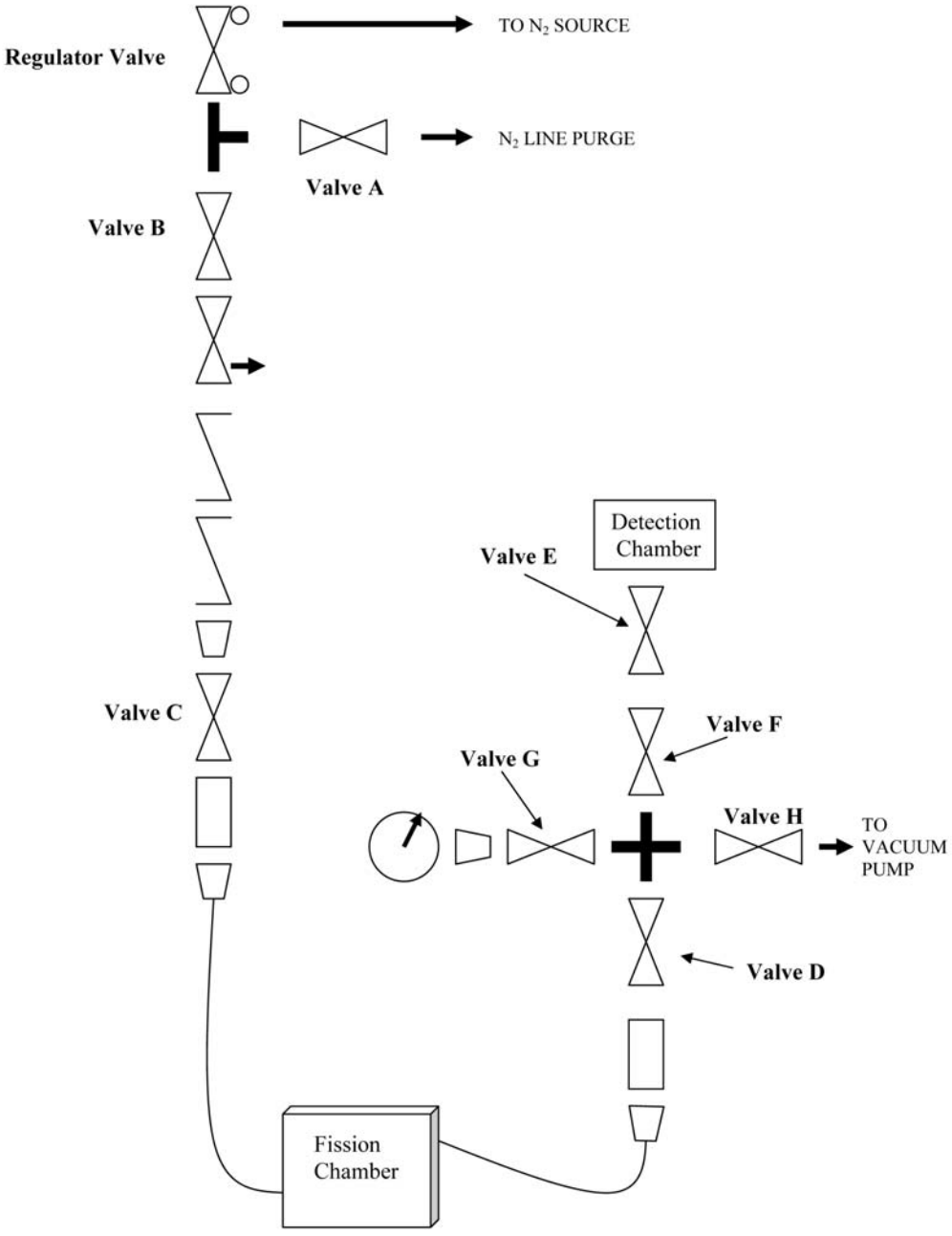

Figure 51) Experiment procedure valve diagram

APPENDIX B – HPGE DETECTOR DOCUMENTATION

QUALITY ASSURANCE DATA SHEET

GEM Series HPGe (High-Purity Germanium) Coaxial Detector System

Model and Serial Numbers

Detector Model No. GEM-30185-P

Cryostat Configuration PopTop

Dewar Model —

Preamplifier Model 237P

Preamplifier S/N #307

H. V. Filter Model 138

H. V. Filter S/N # 7886-3

Important Reference Data

Ship Date 1-10-95

Serial No. 34-TP11105A

When calling Customer Service, always reference this Detector Serial No.

Cryogenic Information

Dewar Capacity — Static Holding Time — Detector Cool-Down Time 6 HRS

Dimensions

Crystal Diameter 56.1 mm

Crystal Length 69.7 mm

End Cap to Crystal 3 mm

Total Active Volume — cc

Absorbing Layers

Aluminum 1.27 mm

Magnesium — mm

Inactive Germanium 700 ~~mm~~

High Voltage Bias

Recommended Operation Bias, POSITIVE 2000 V

Performance Specifications*

	Warranted	Measured	Amplifier Time Constant
Resolution (FWHM) at 1.33 MeV, ^{60}Co	1.85 keV	1.72 keV	6 us
Peak-to-Compton Ratio, ^{60}Co	58	64.6	6 us
Relative Efficiency at 1.33 MeV, ^{60}Co	30 %	33.6 %	6 us
Peak Shape (FWTM/FWHM), ^{60}Co	1.90	1.87	6 us
Peak Shape (FWFM/FWHM), ^{60}Co	2.65	2.52	6 us
Resolution (FWHM) at 122 kev, ^{57}Co	875 eV	769 eV	

Other Capsule SCA #3546

Cryo PH-2 #3852

Data Certified By Glanagan Date 1-10-95

*Measured at a nominal rate of 1000 counts/s unless otherwise specified.

APPENDIX C – DETAILED CHAMBER DRAWINGS

Drawings created using the Solid Works program. All dimensions are listed in inches.

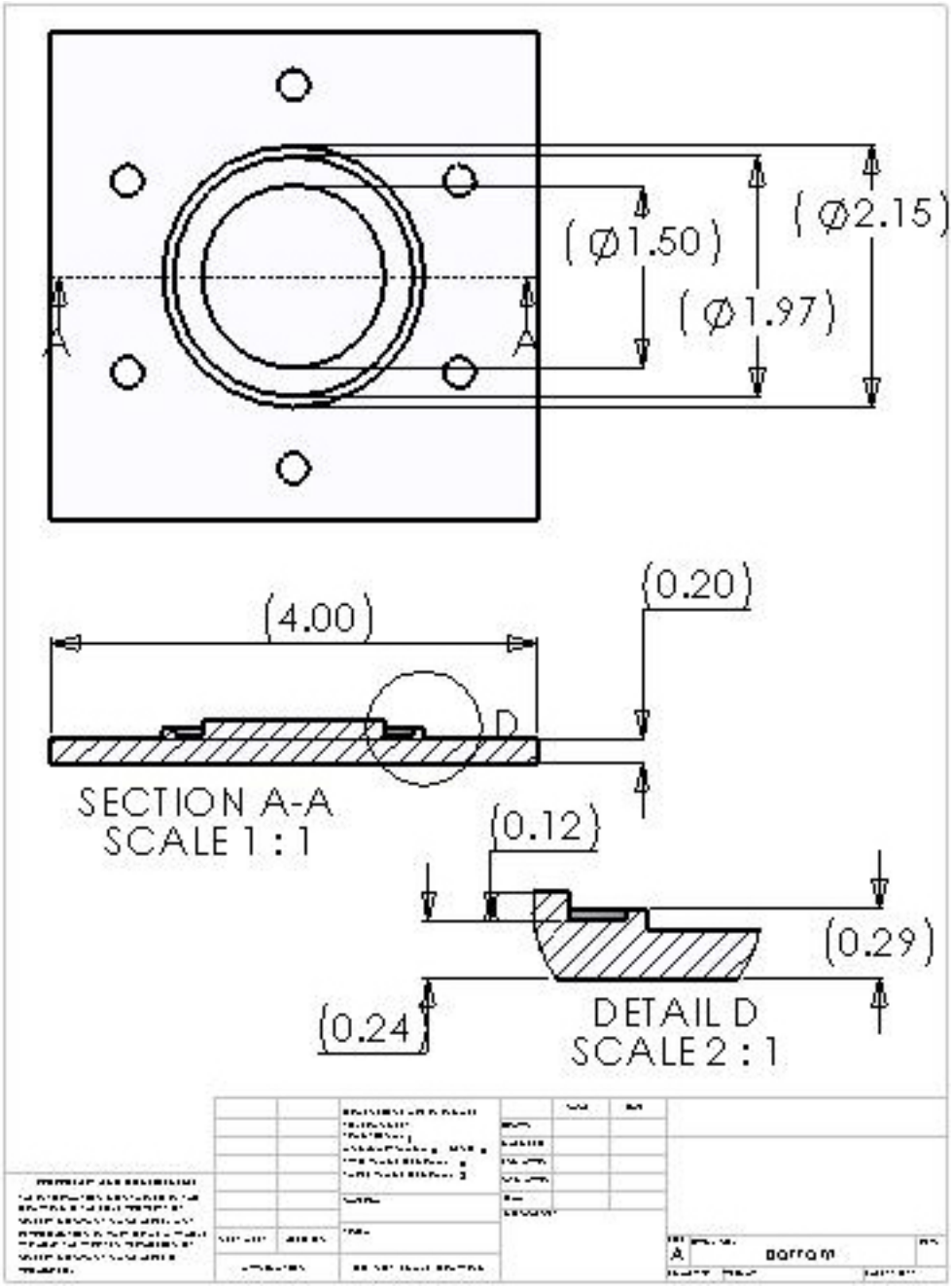

Figure 52) Chamber bottom detailed drawing complete view

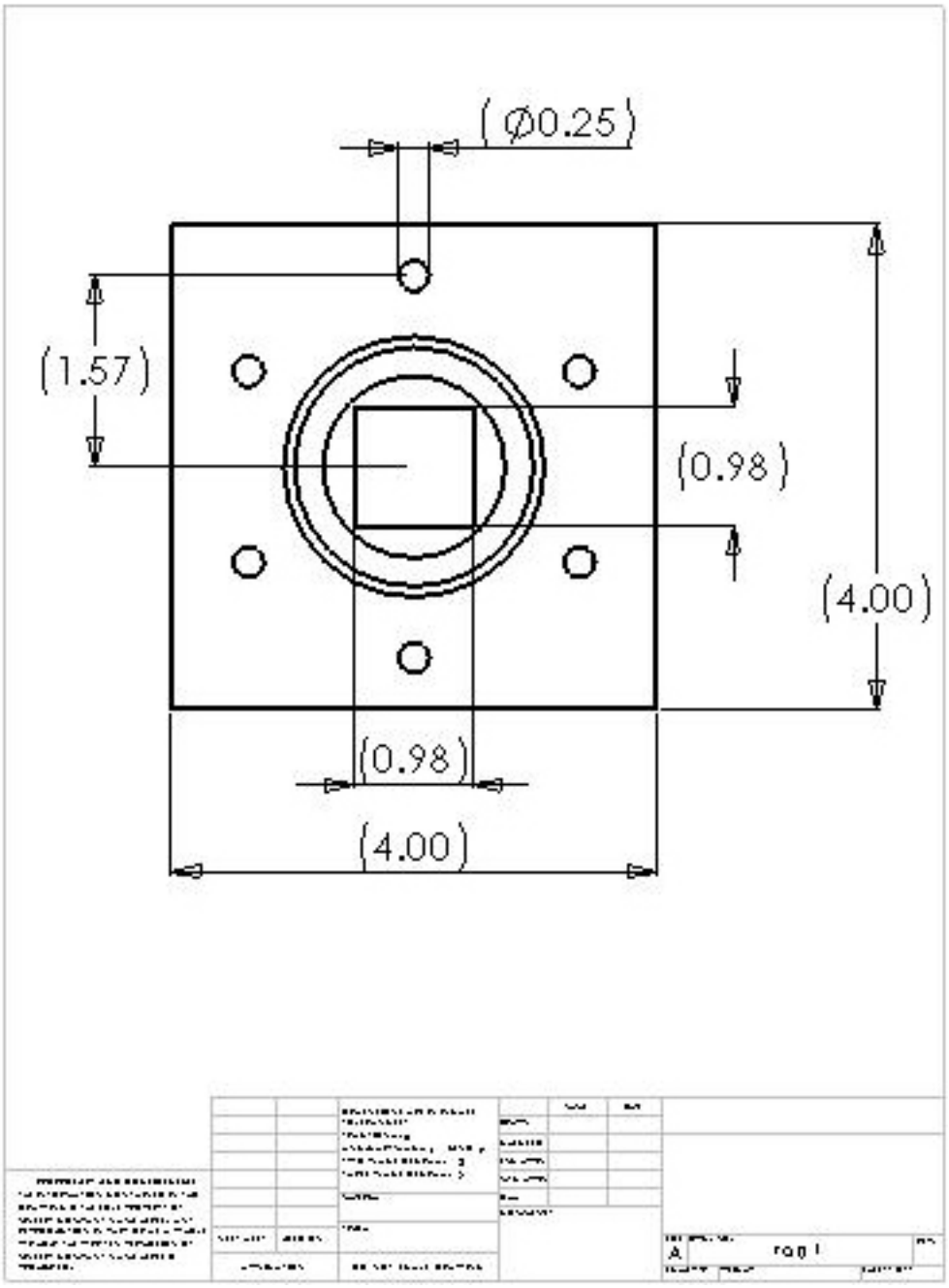

Figure 53) Chamber top detailed drawing top view

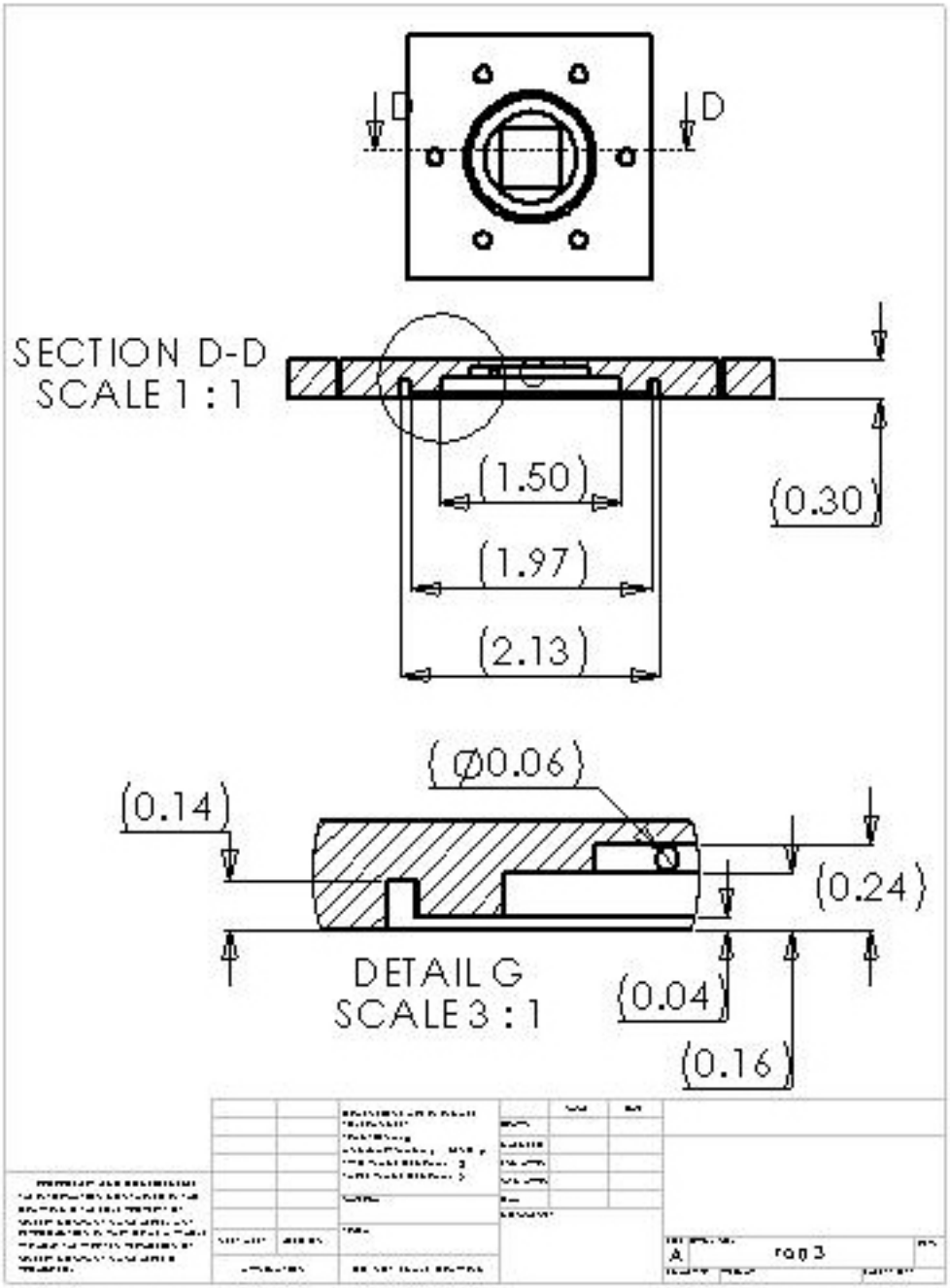

Figure 54) Chamber top detailed drawing side view

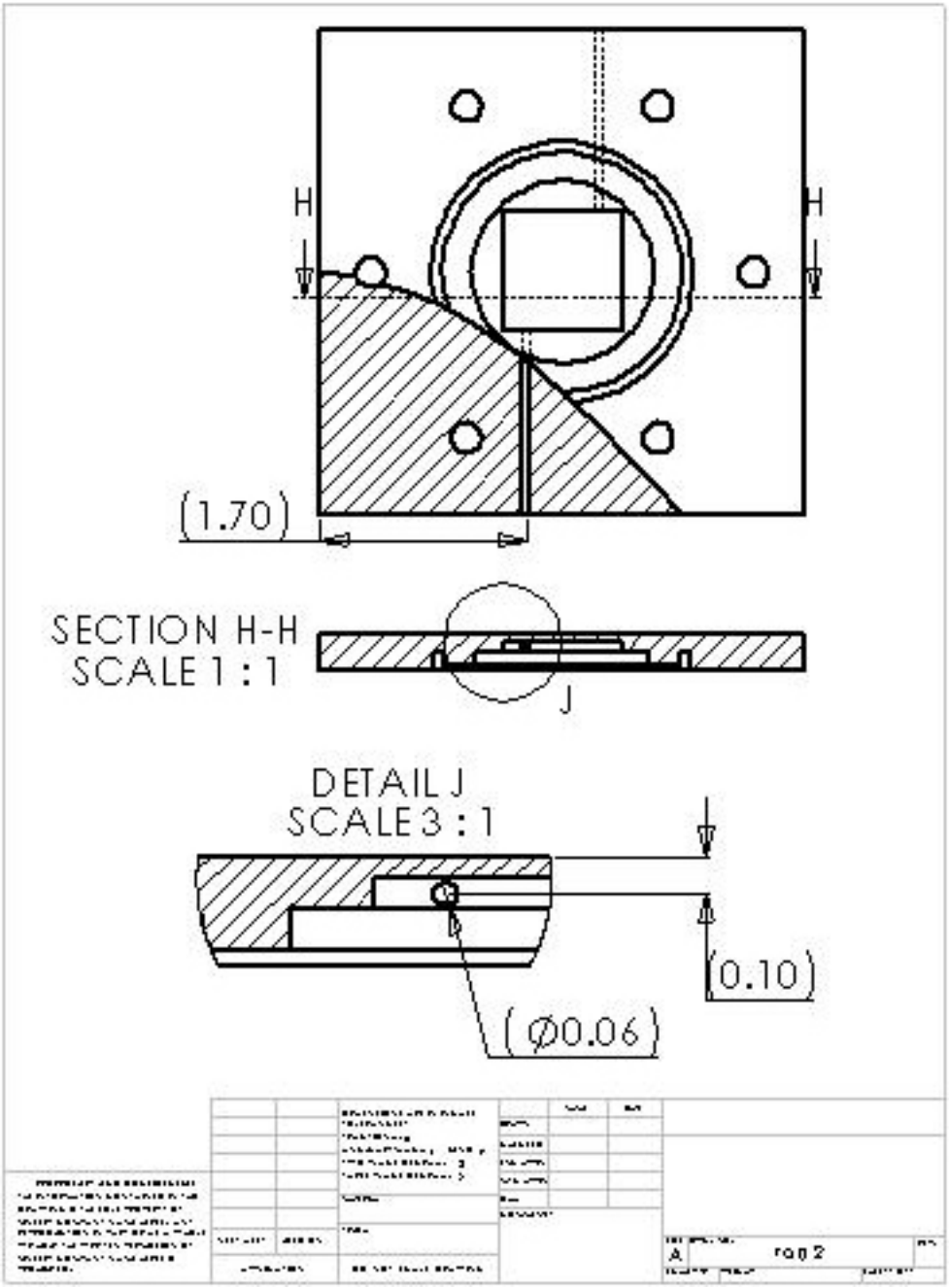

Figure 55) Chamber top detailed drawing mircotubing view

APPENDIX D – FISSION YIELDS

Thermal Neutron Induced Fission. Data from T.R. England and B.F. Rider, Los Alamos National Laboratory, LA-UR-94-3106; ENDF-349 (1993).

Table 11) 131 decay chain cumulative and independent yield data

131 Decay Chain			
Isotope	Half-life	Independent Yield	Cumulative Yield
^{131}Cd	0.106 sec	1.38E-02	1.38E-02
^{131}In	0.28 sec	1.11E-02	2.49E-02
^{131}Sn	39 sec	8.81E-01	9.06E-01
^{131}Sb	23 min	1.65E+00	2.56E+00
^{131m}Te	1.35 days	2.33E-01	4.12E-01
^{131}Te	25 min	9.70E-02	2.55E+00
^{131}I	8.04 days	3.92E-03	2.89E+00
^{131m}Xe	11.9 days	3.48E-07	4.05E-02
^{131}Xe	Stable		

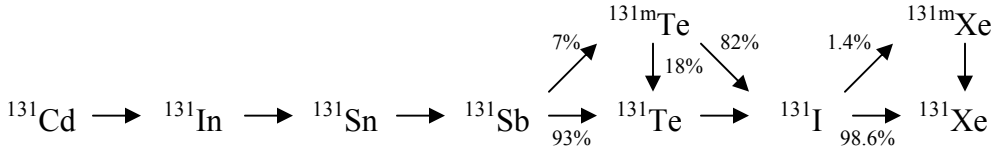

Figure 56) 131 decay chain schematic

Table 12) 133 decay chain cumulative and independent yield data

133 Decay Chain			
Isotope	Half-life	Independent Yield	Cumulative Yield
^{133}In	0.18 sec	1.71E-04	1.71E-04
^{133}Sn	1.44 sec	1.38E-01	1.38E-01
^{133}Sb	2.5 min	2.26E+00	2.40E+00
^{133m}Te	55.4 min	2.99E+00	3.99E+00
^{133}Te	12.4 min	1.15E+00	3.06E+00
^{133}I	20.8 hr	1.65E-01	6.70E+00
^{133m}Xe	2.19 days	1.89E-03	1.89E-01
^{133}Xe	5.243 days	6.66E-04	6.70E+00
^{133}Cs	Stable		

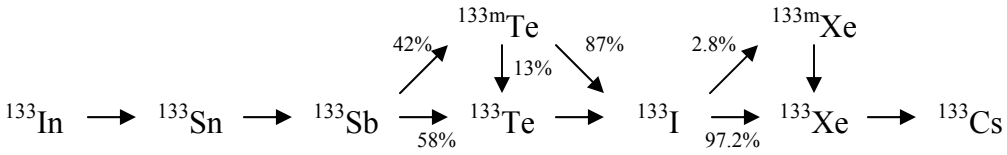

Figure 57) 131 decay chain schematic

Table 13) 135 decay chain cumulative and independent yield data

135 Decay Chain			
Isotope	Half-life	Independent Yield	Cumulative Yield
^{135}Sn	0.418 sec	6.27E-04	6.27E-04
^{135}Sb	1.71 sec	1.45E-01	1.46E-01
^{135}Te	19 sec	3.22E+00	3.34E+00
^{135}I	6.57 hr	2.93E+00	6.28E+00
^{135m}Xe	15.3 min	1.78E-01	1.10E+00
^{135}Xe	9.1 hr	7.85E-02	6.54E+00
^{135}Cs	2300000 yr	4.91E-04	6.54E+00
^{135}Ba	Stable		

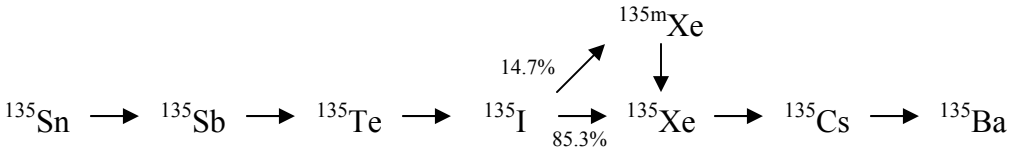

Figure 58) 131 decay chain schematic

APPENDIX E – CD WITH ALL FILES

a) **EXCEL Irradiation Time Calculation**

b) **SOLID WORKS Drawings**

c) **STELLA Program**

APPENDIX F – IRRADIATION LOG

The following information in **Table 14** is an irradiation log that will be amended after subsequent irradiation of the HEU foil has occurred.

Table 14) Irradiation Log

Irradiation	Time/Date	Irradiation Duration	Build In Time
1	3:00 pm 5/9/08	20 minutes	67 hours
2			
3			
4			
5			